US010690517B2

(12) **United States Patent**
Qama et al.

(10) **Patent No.: US 10,690,517 B2**
(45) **Date of Patent: Jun. 23, 2020**

(54) **SENSOR COIL OPTIMIZATION**

(71) Applicant: **Integrated Device Technology, Inc.**, San Jose, CA (US)

(72) Inventors: **Gentjan Qama**, Munich (DE); **Mauro Passarotto**, Anguillara Veneta (IT); **Ruben Specogna**, Pagnacco (IT)

(73) Assignee: **Integrated Device Technology, Inc.**, San Jose, CA (US)

(*) Notice: Subject to any disclaimer, the term of this patent is extended or adjusted under 35 U.S.C. 154(b) by 0 days.

(21) Appl. No.: **16/024,298**

(22) Filed: **Jun. 29, 2018**

(65) **Prior Publication Data**

US 2019/0128702 A1 May 2, 2019

Related U.S. Application Data

(60) Provisional application No. 62/580,354, filed on Nov. 1, 2017.

(51) **Int. Cl.**
G01R 33/00 (2006.01)
G01D 5/20 (2006.01)

(52) **U.S. Cl.**
CPC ***G01D 5/2046*** (2013.01); ***G01D 5/2053*** (2013.01); ***G01D 5/2073*** (2013.01); ***G01R 33/0017*** (2013.01)

(58) **Field of Classification Search**
CPC .. G01D 5/2046; G01D 5/2053; G01D 5/2073; G01R 33/0017
USPC 324/207.17
See application file for complete search history.

(56) **References Cited**

U.S. PATENT DOCUMENTS

8,421,447 B2 * 4/2013 Inoue G01B 7/003 324/207.16
8,928,311 B2 * 1/2015 Sasaki G01D 5/2073 324/207.17
2014/0218036 A1 8/2014 Fry
2015/0339421 A1 11/2015 Srinivasan et al.

FOREIGN PATENT DOCUMENTS

EP 1975570 B1 10/2014

OTHER PUBLICATIONS

Bettini et al., "A Boundary Integral Method for Computing Eddy Currents in Thin Conductors for Arbitrary Topology," IEEE Transactions on Magnetics, vol. 41, No. 3. 2015. 4 pages.
Bettini et al., "A Volume Integral Formulation for Solving Eddy Current Problems on Polyhedral Messes," IEEE Transactions on Magnetics, vol. 53, No. 6. 2017. 4 pages.
S. Rao, "Engineering Optimization: Theory and Practice," John Wiley & Sons, 4th edition, 2009. 830 pages.
(Continued)

Primary Examiner — Reena Aurora
(74) *Attorney, Agent, or Firm* — Haynes and Boone, LLP

(57) **ABSTRACT**

In some embodiments, a coil design system is provided. In particular, a method of providing an optimized position locating sensor coil design in presented. The method includes receiving a coil design; simulating position determination with the coil design to form a simulated performance; comparing the simulated response with the specification to provide a comparison; and modifying the coil design based on a comparison between the simulated performance and a performance specification to arrive at an updated coil design.

19 Claims, 24 Drawing Sheets

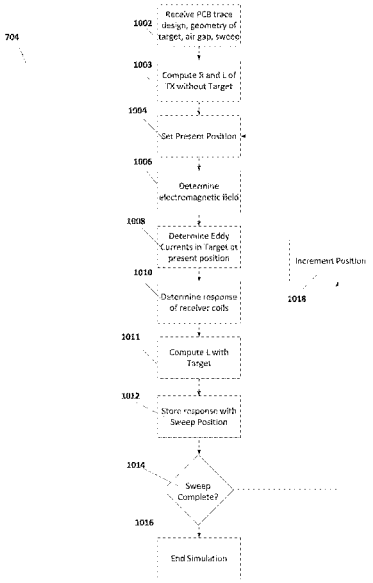

(56) **References Cited**

OTHER PUBLICATIONS

Palit, A.K., "Frequency Response Modeling of Inductive Position Sensor with Finite Element Tools," from the Proceedings of the 2014 COMSOL Conference in Cambridge (2014), pg. 1, col. 2, para 2-3; p. 3, col. 1, para 1-2; p. 4, col 1, para 1; p. 5, col. 1, para 1; p. 5, col. 2, para 1; Fig 1, 4, 8. Available Online at: https://www.comsol.com/paper/download/199331/palit_paper.pdf. pp. 1-4.

Aschenbrenner et al., "Contactless High Frequency Inductive Position Sensor with DSP Read Out Electronics Utilizing Band-Pass Sampling," ACTA IMEKO, 3(3) p. 50-56, Sep. 2014, abstract; p. 50, col. 2, para 1, 4: p. 51, col 2, para 1; Fig 2. Available Online at: https://actaimeko.org/index.php/acta-imeko/issue/view/8/showToc.

International Search Report issued by the International Searching Authority dated Nov. 9, 2018 for PCT Application No. PCT/US2018/041124. pp. 1-4.

Written Opinion issued by the International Searching Authority dated Nov. 9, 2018 for PCT Application No. PCT/US2018/041124. pp. 1-7.

* cited by examiner

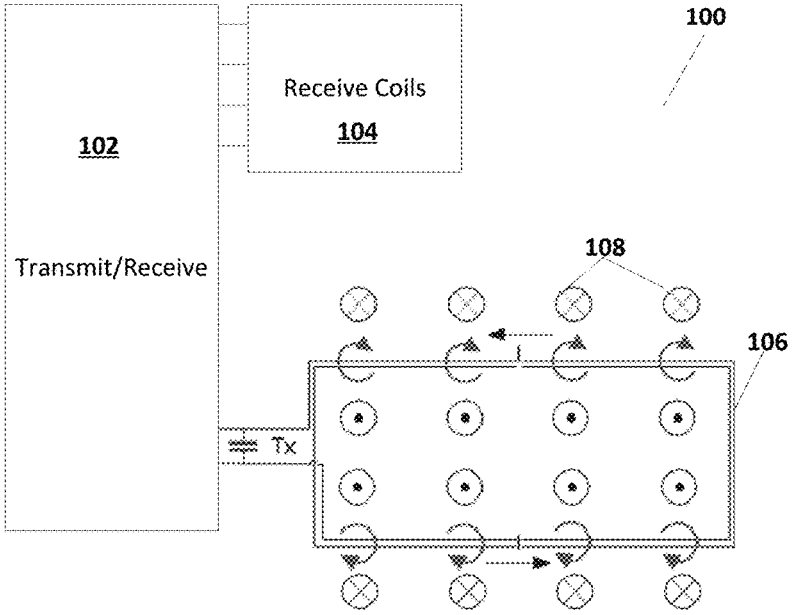

Figure 1A

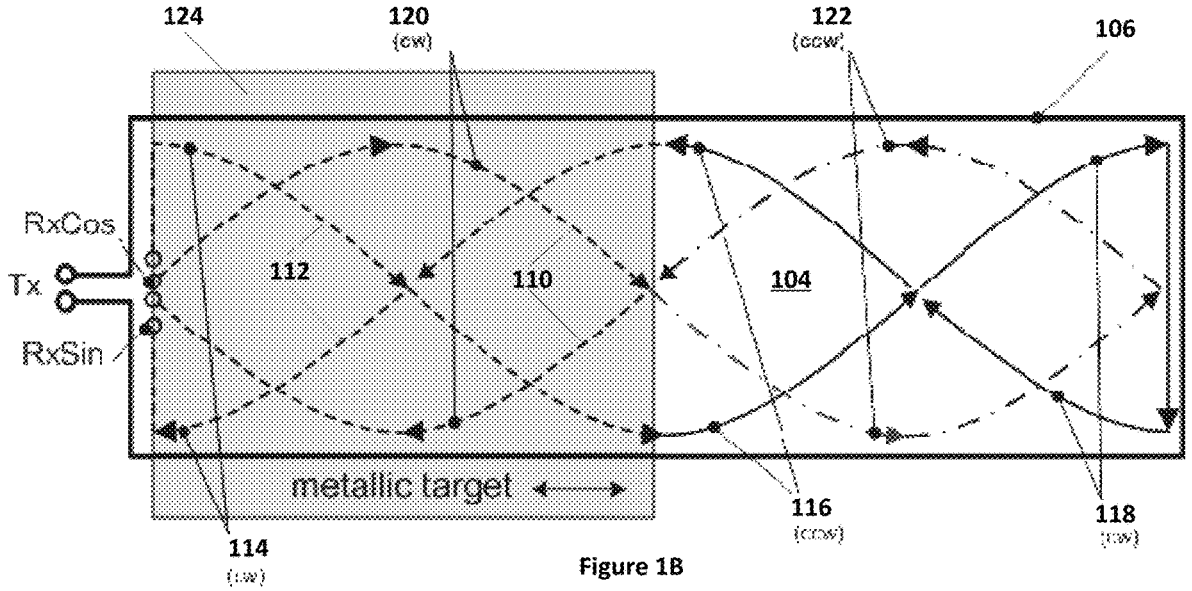

Figure 1B

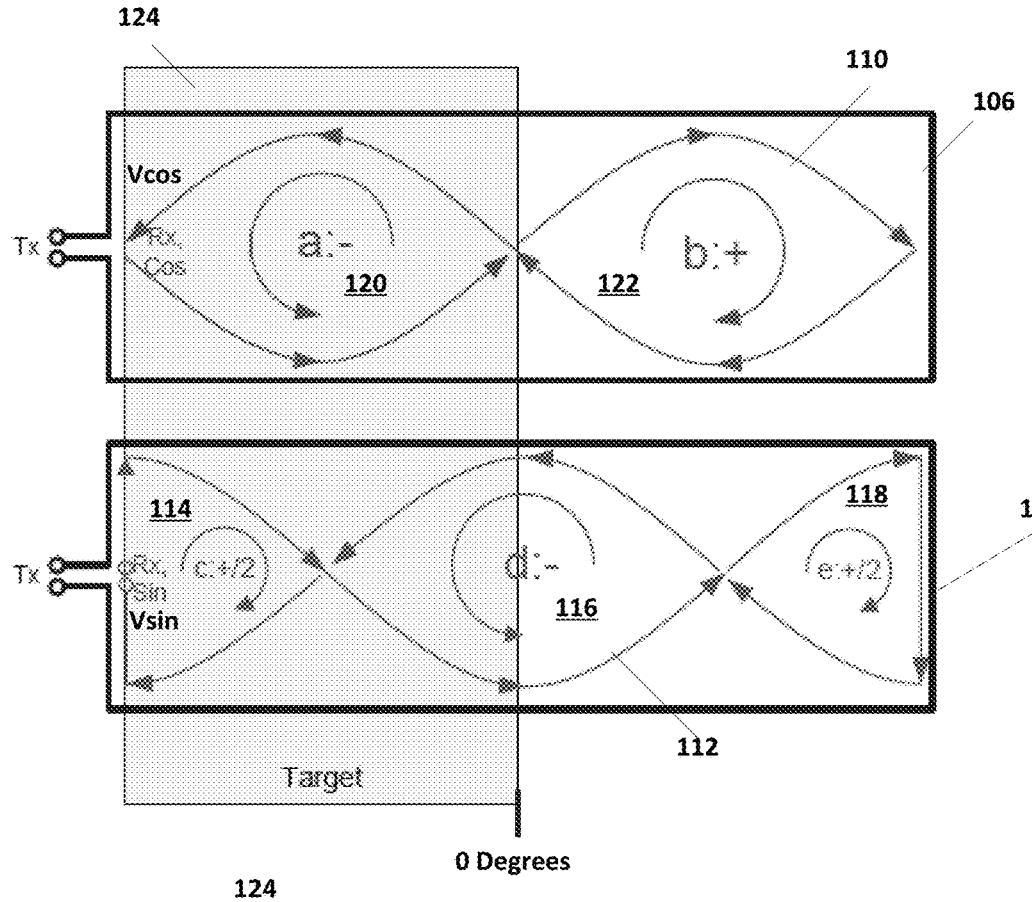

Figure 2A

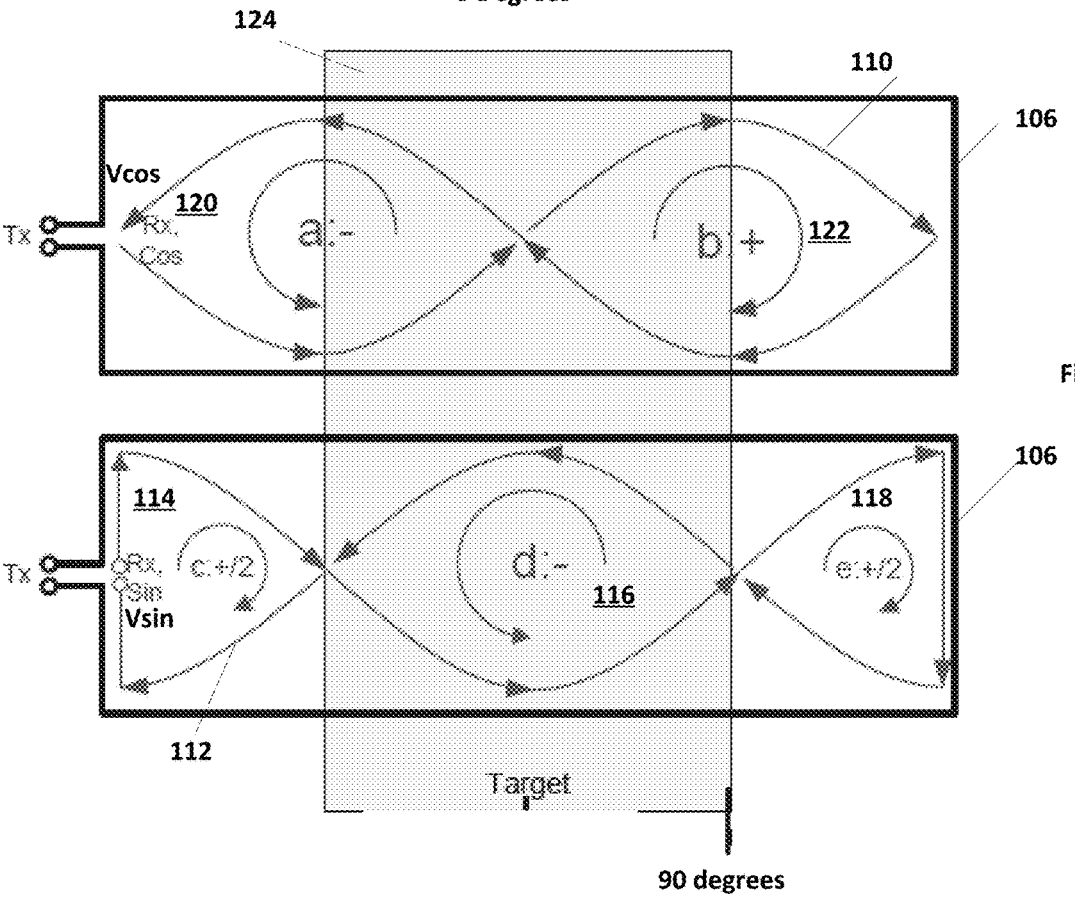

Figure 2B

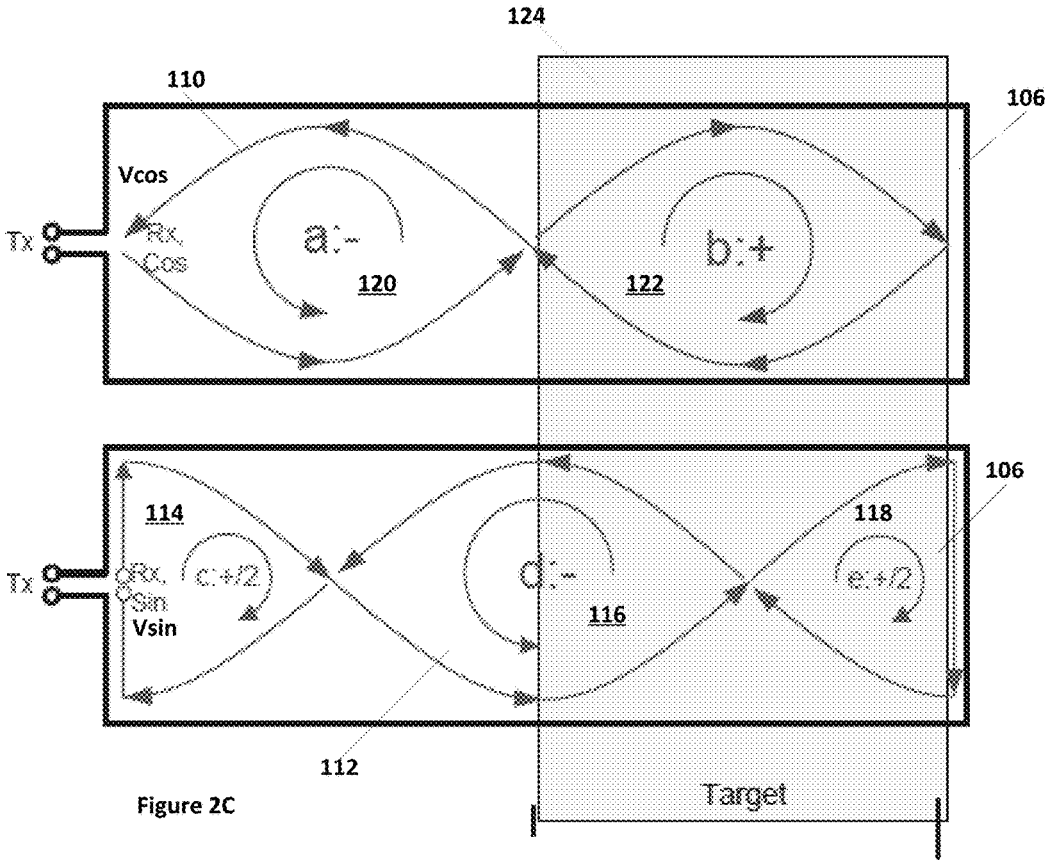

Figure 2C

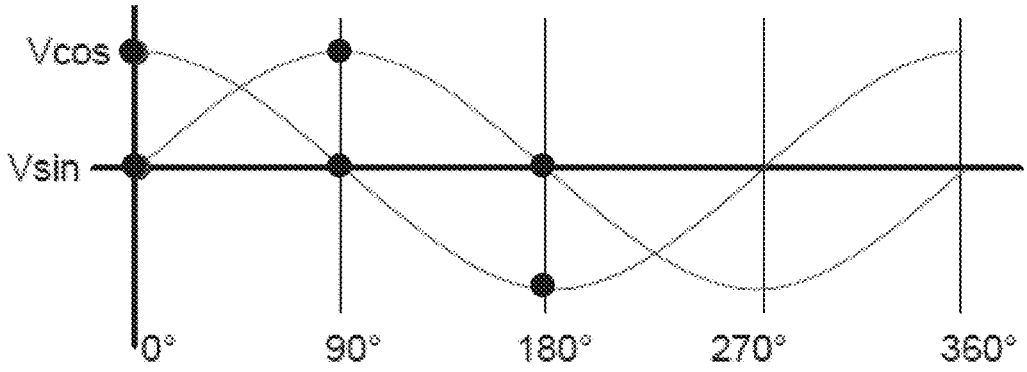

Figure 2D

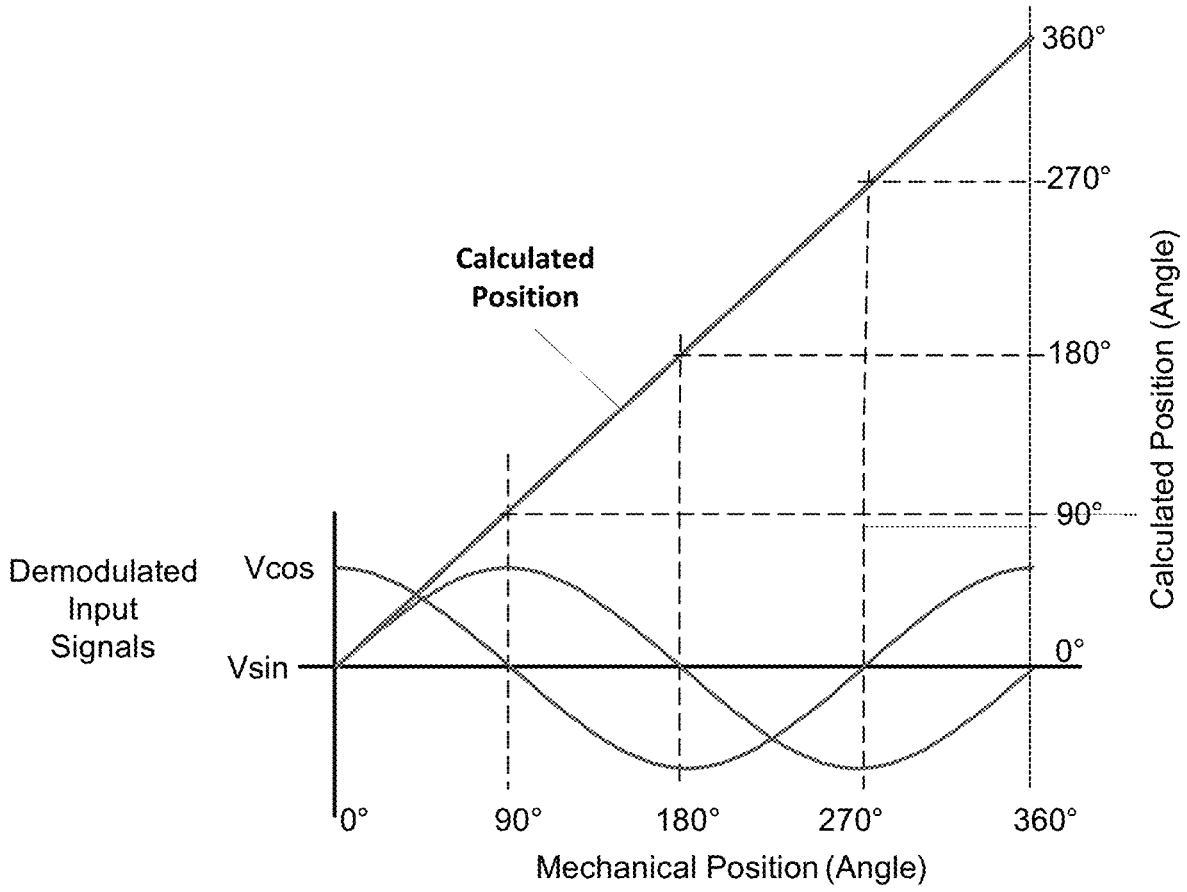
360°
270°
180°
90°
0°
Calculated Position
Calculated Position (Angle)
Demodulated Input Signals
Vcos
Vsin
0°
90°
180°
270°
360°
Mechanical Position (Angle)

Figure 2E

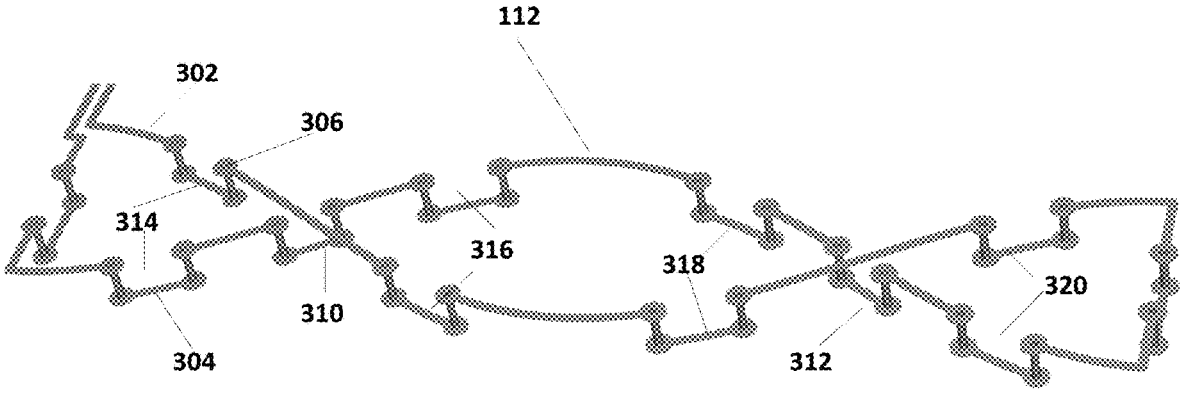

Figure 3A

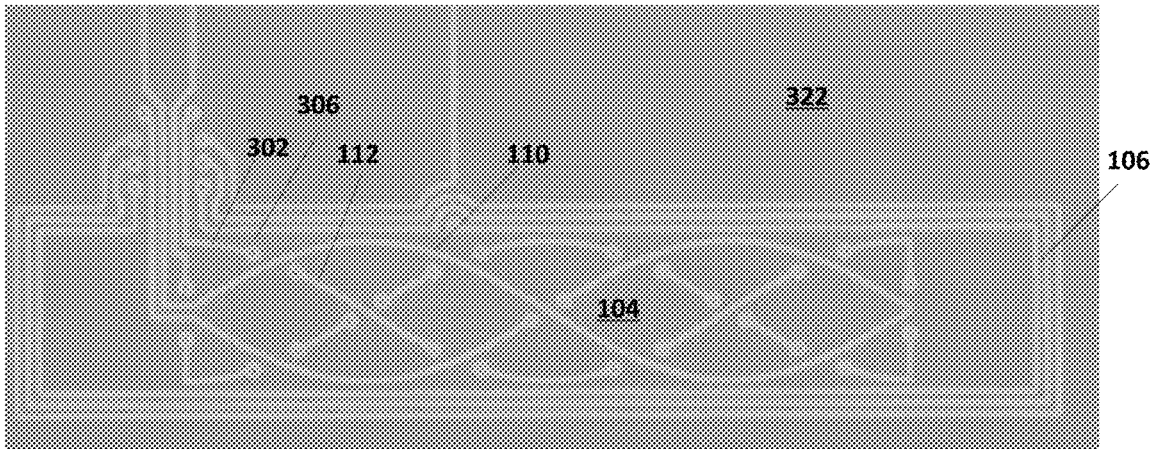

Figure 3B

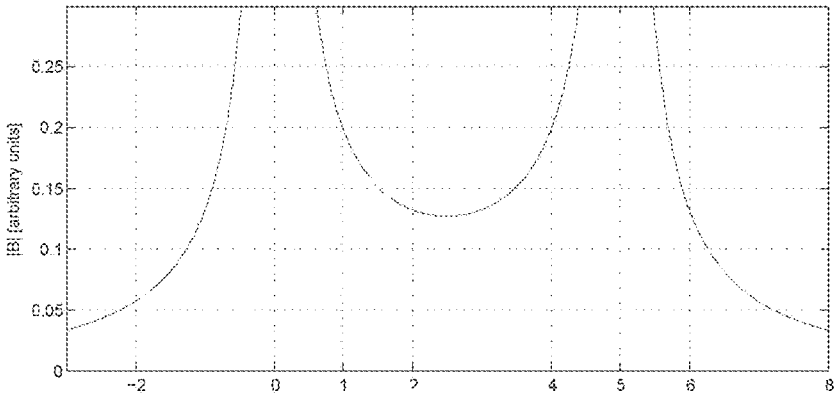

Figure 3C

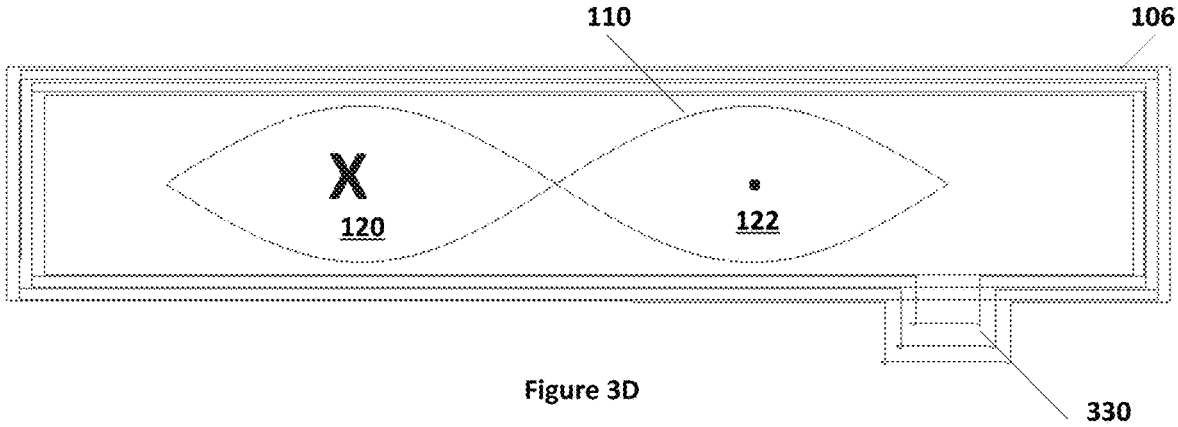

Figure 3D

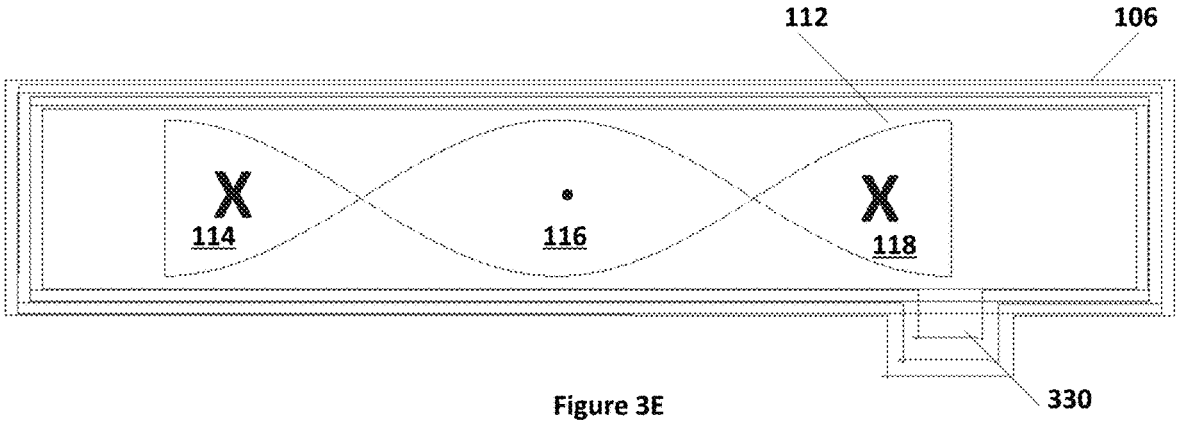

Figure 3E

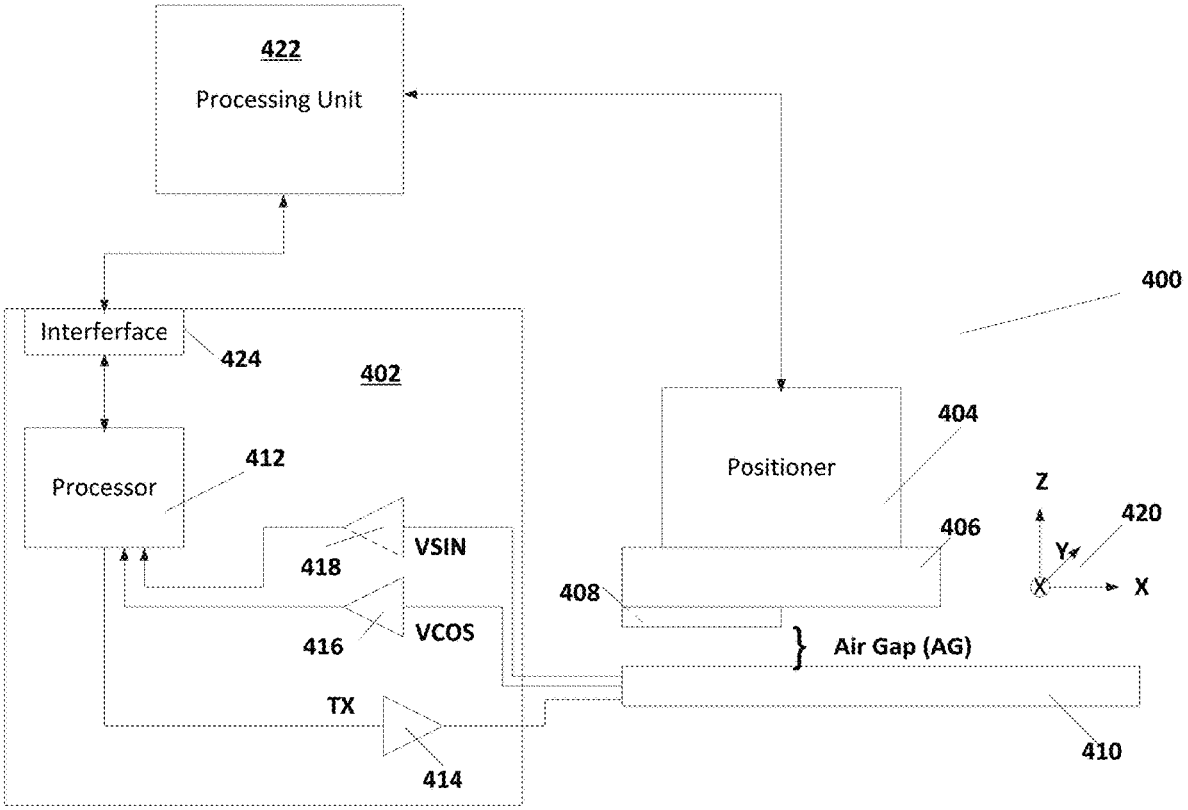

Figure 4A

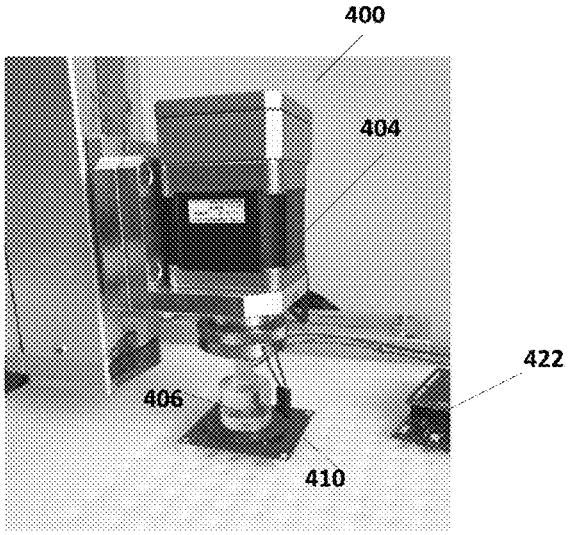

Figure 4B

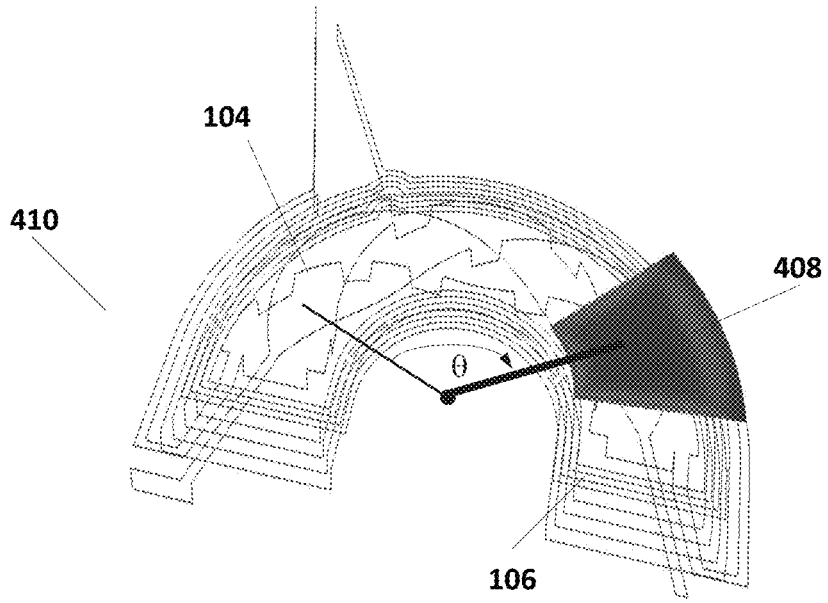

Figure 4C

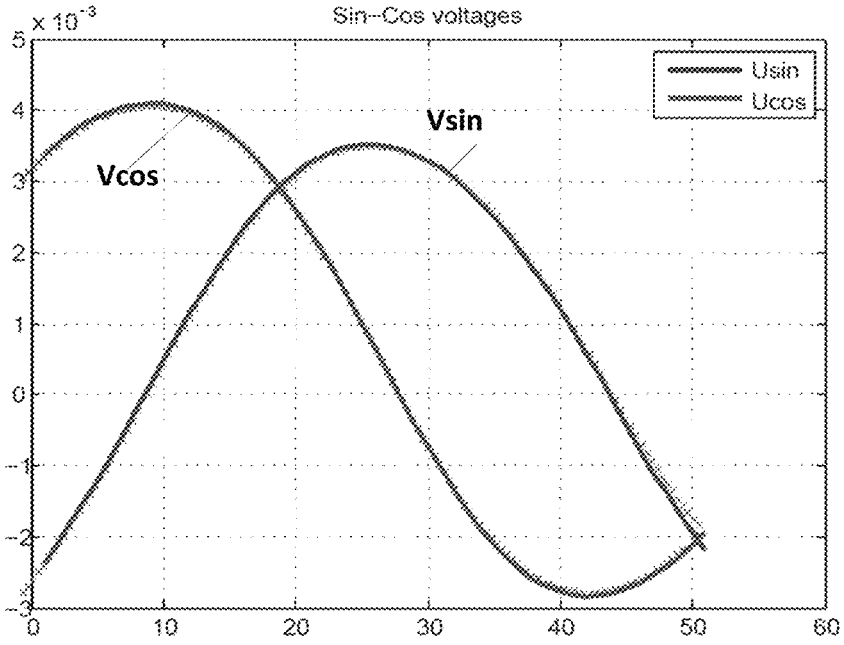

Figure 4D

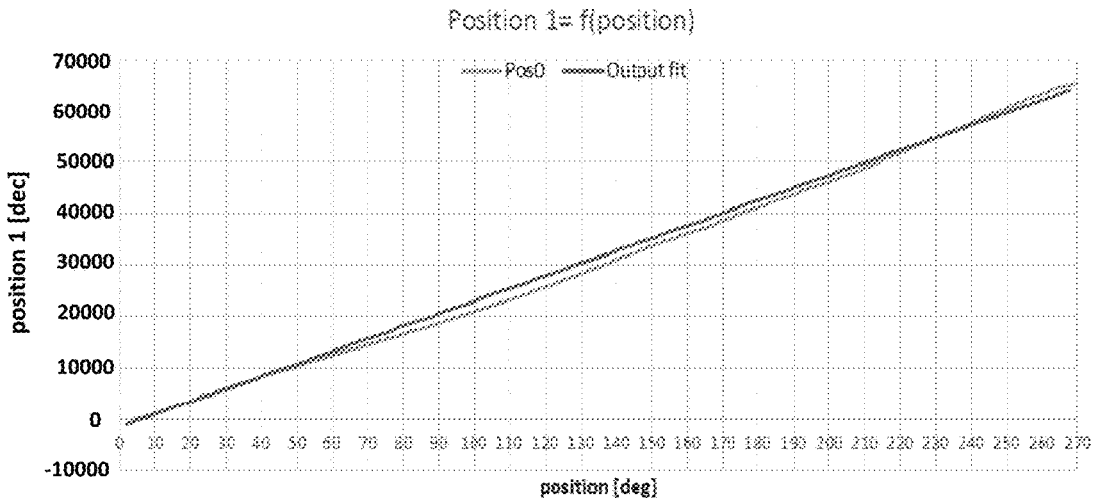

Figure 5

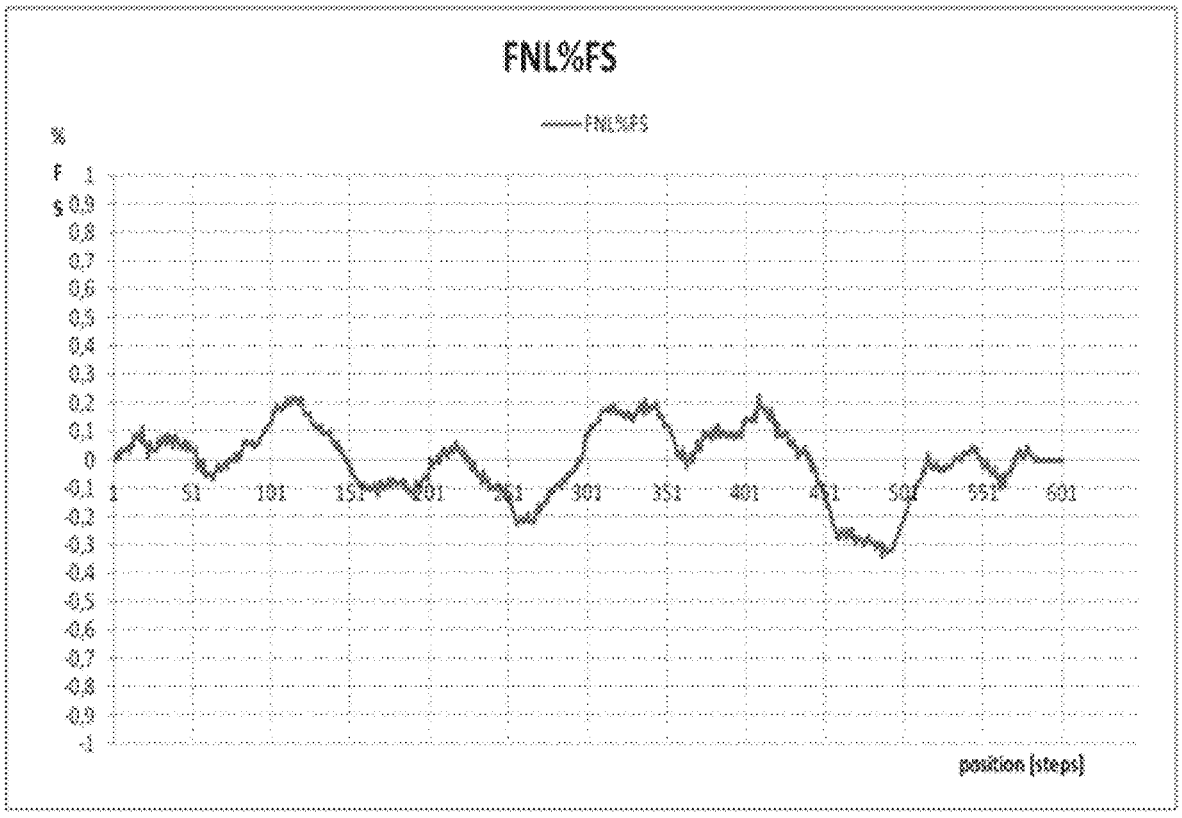

Figure 6

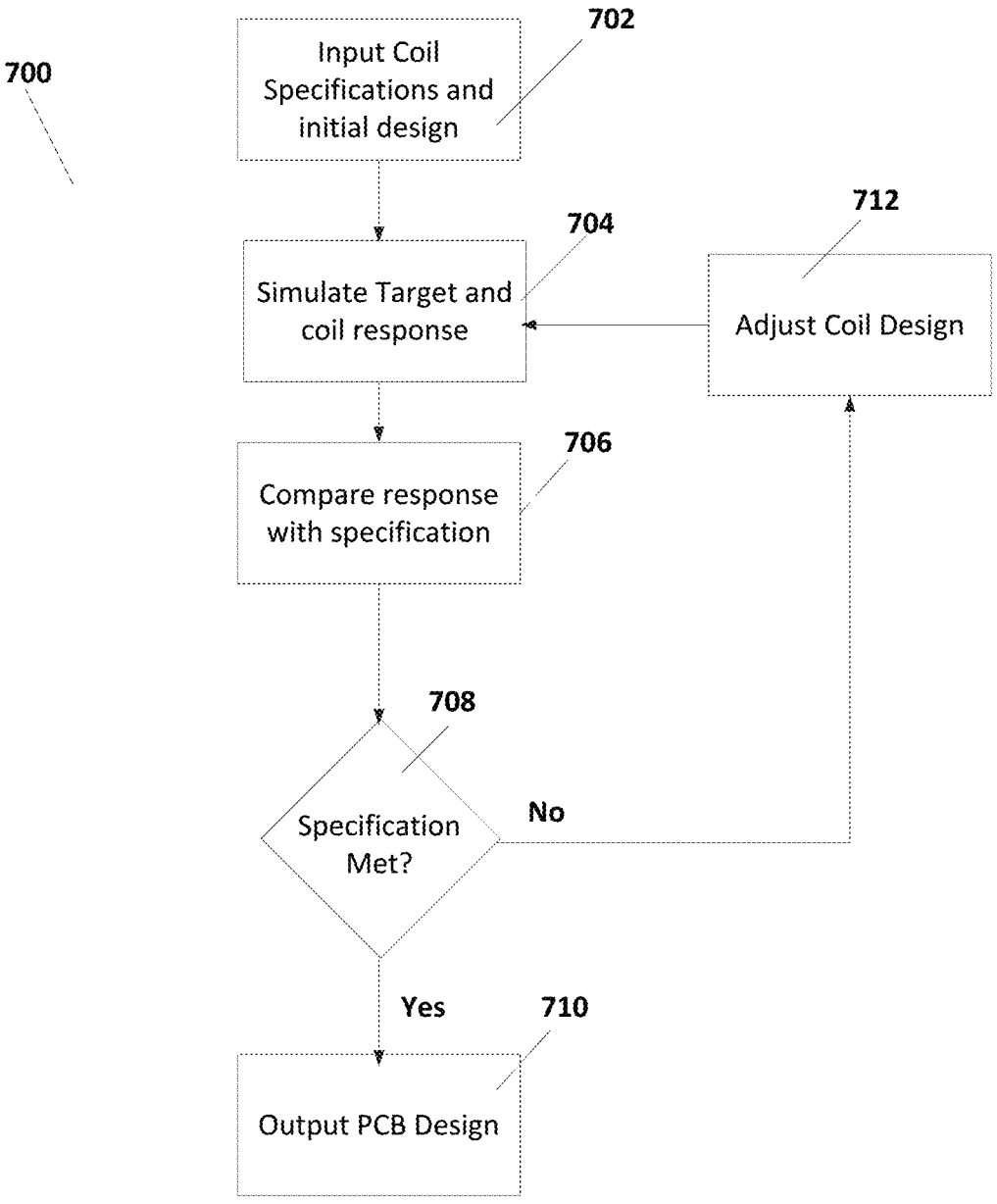
700
Input Coil Specifications and initial design
702
Simulate Target and coil response
704
Adjust Coil Design
712
Compare response with specification
706
Specification Met?
708
No
Yes
Output PCB Design
710

Figure 7A

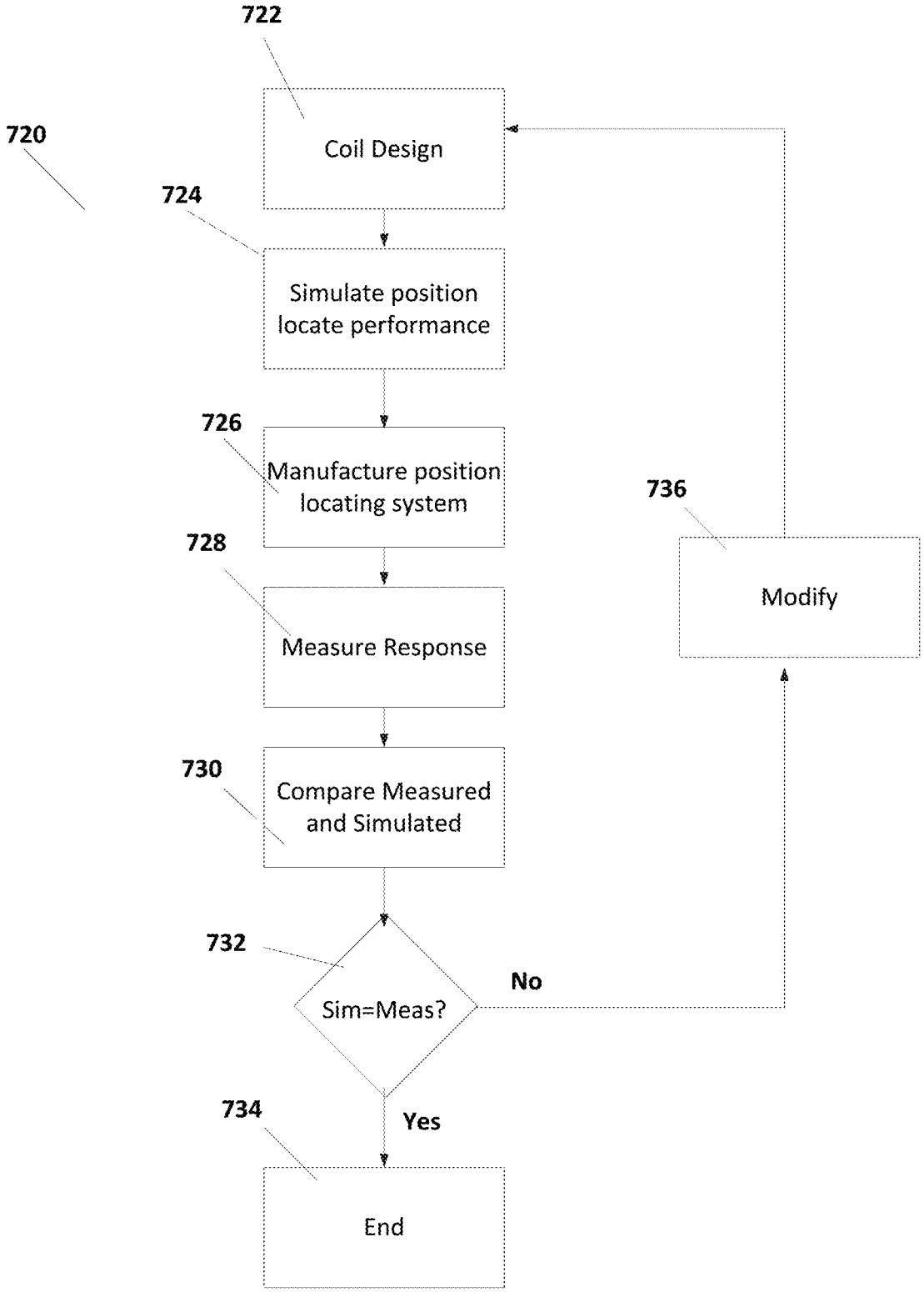
722
720
Coil Design
724
Simulate position locate performance
726
Manufacture position locating system
736
728
Modify
Measure Response
730
Compare Measured and Simulated
732
Sim=Meas?
No
734
Yes
End

Figure 7B

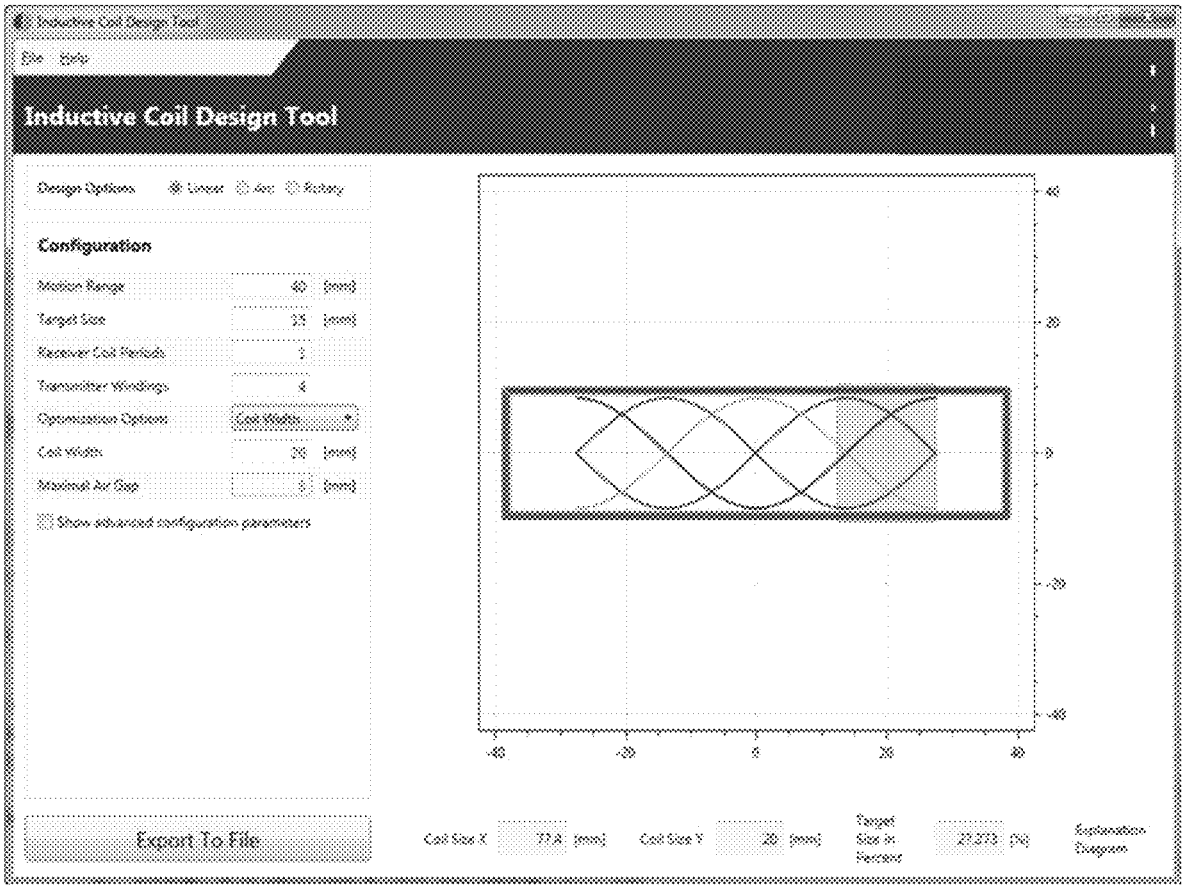

Figure 7C

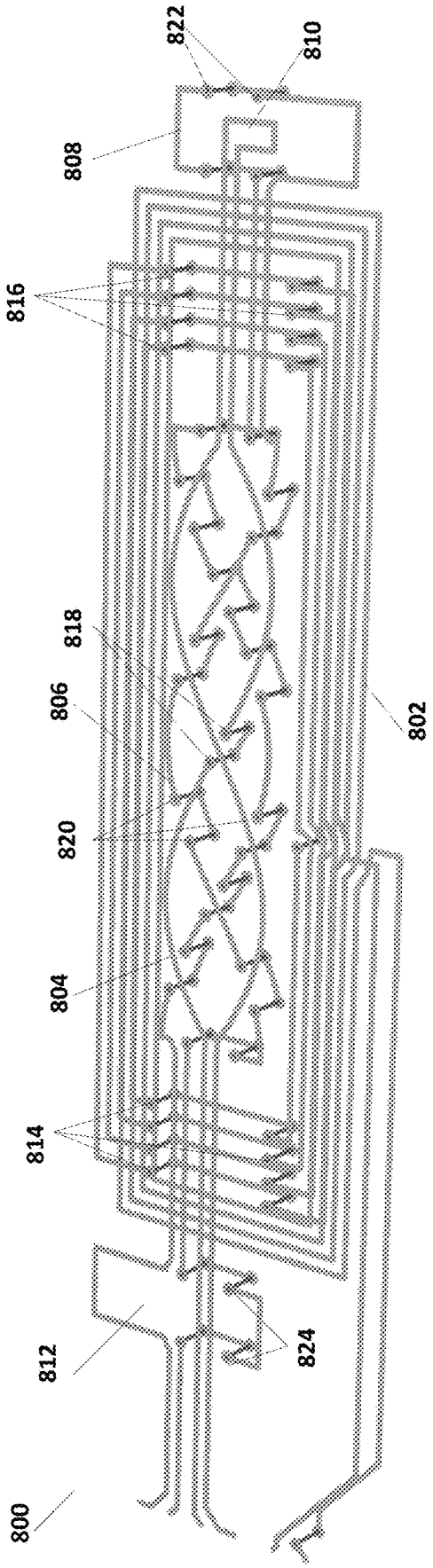

Figure 8A

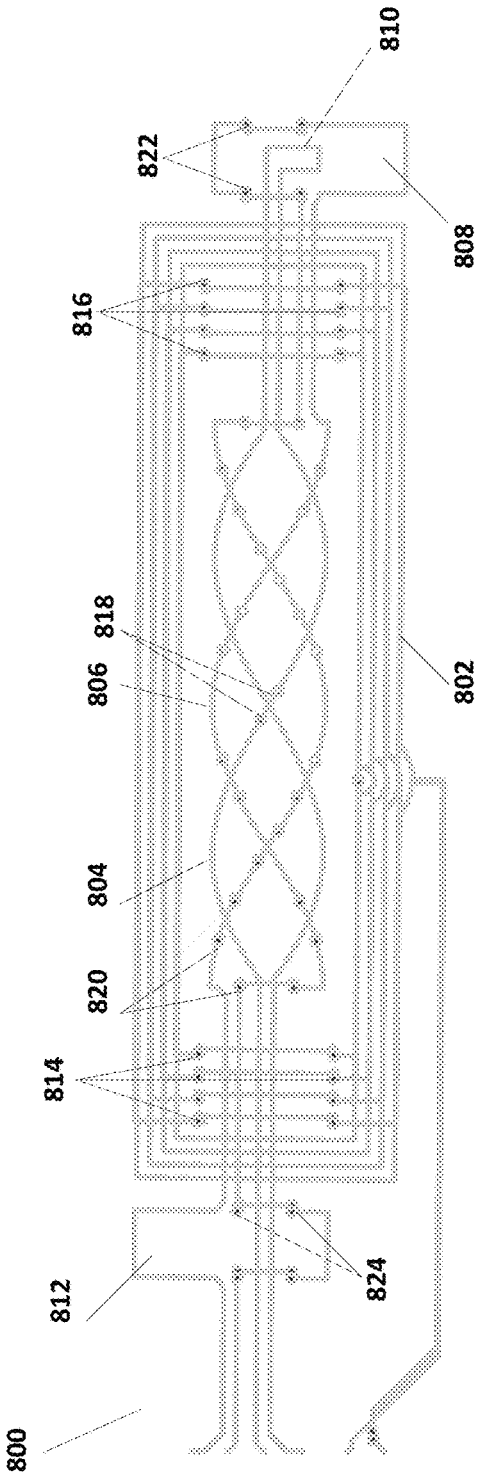

Figure 8B

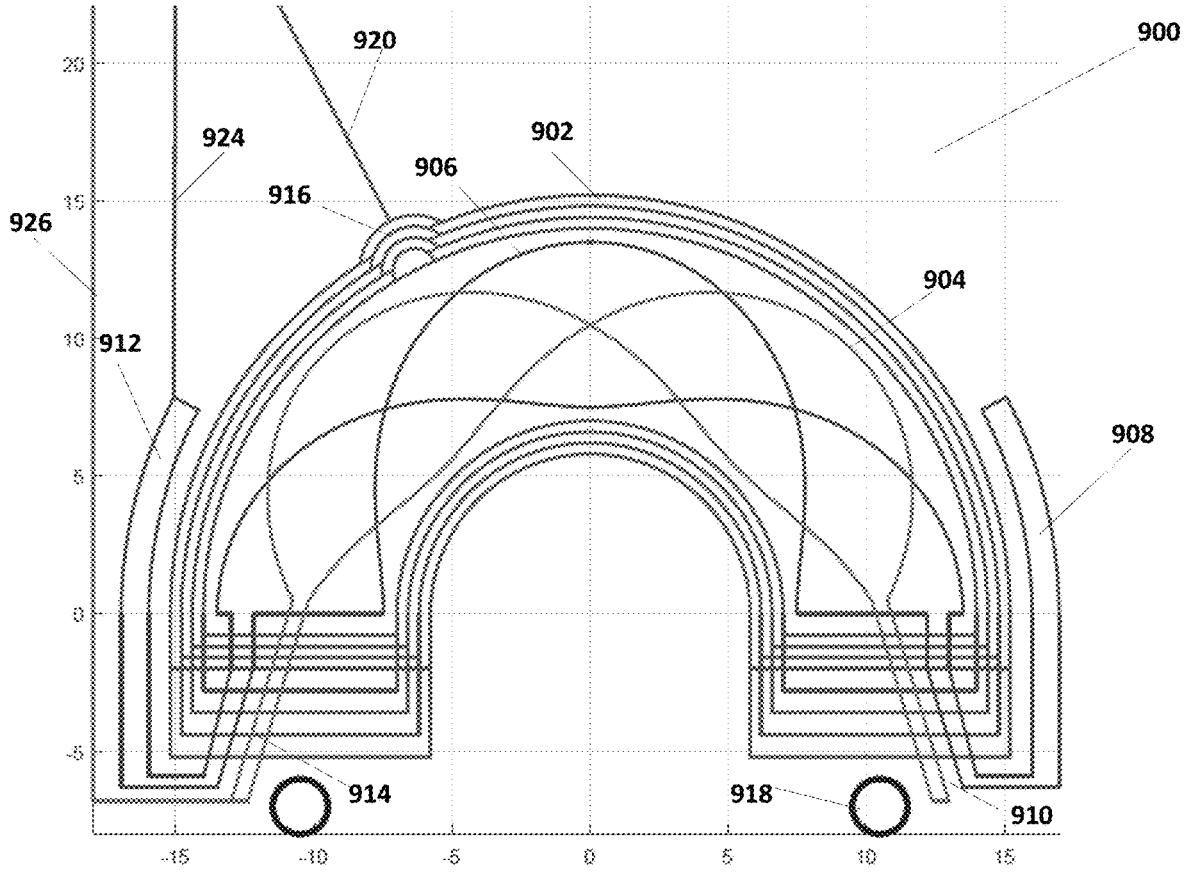

Figure 9A

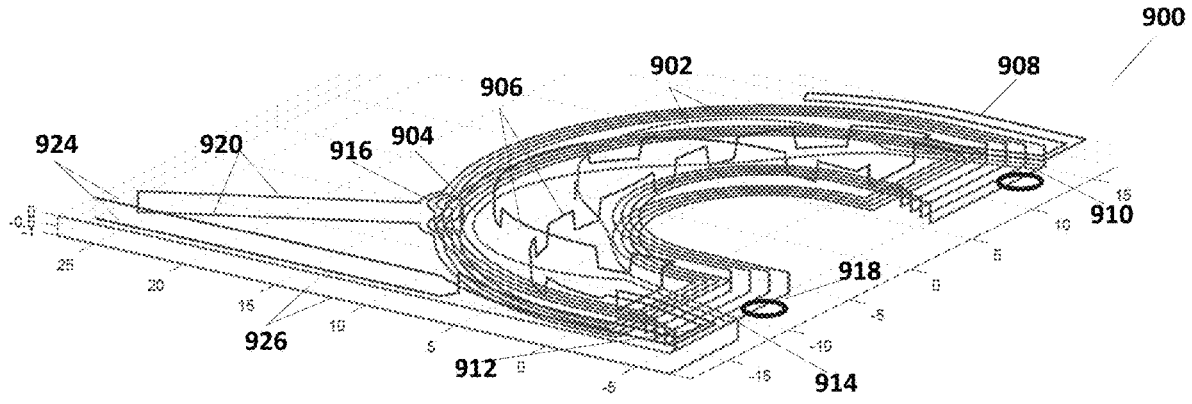

Figure 9B

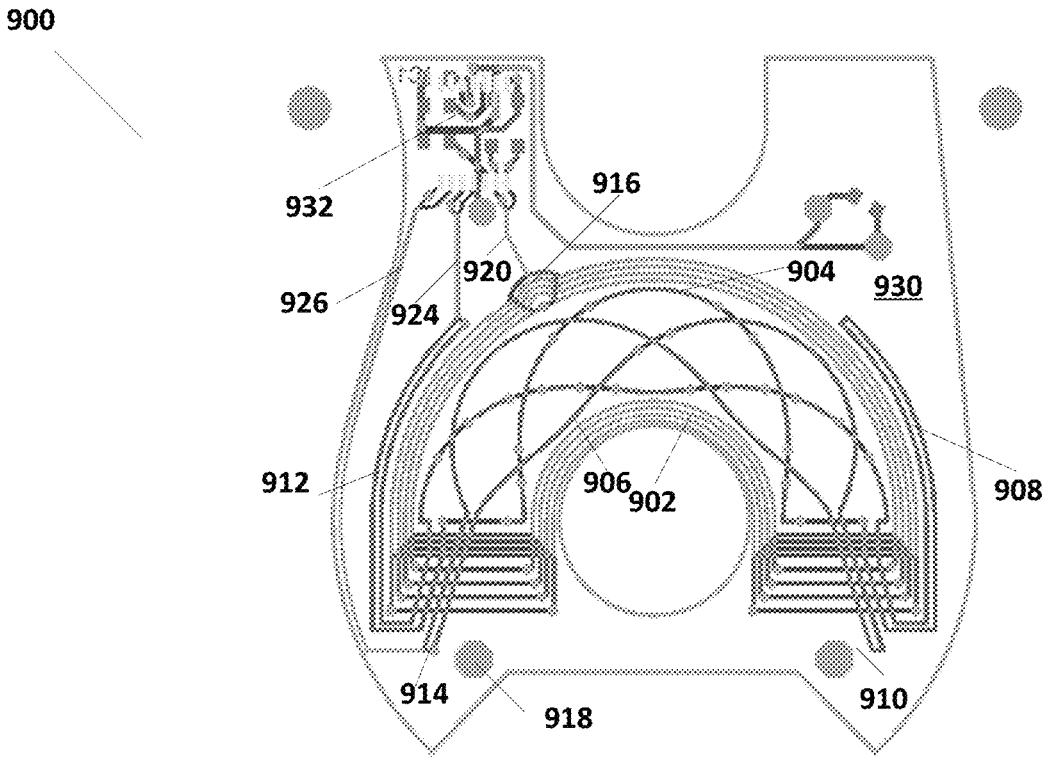

Figure 9C

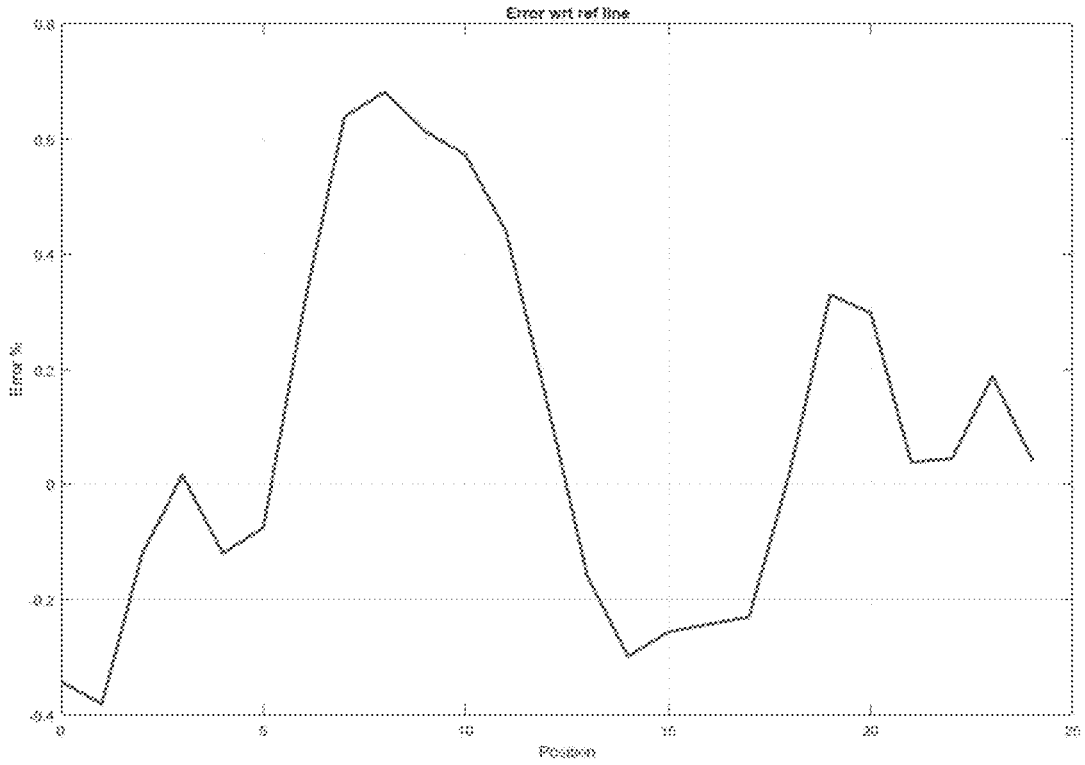

Figure 9D

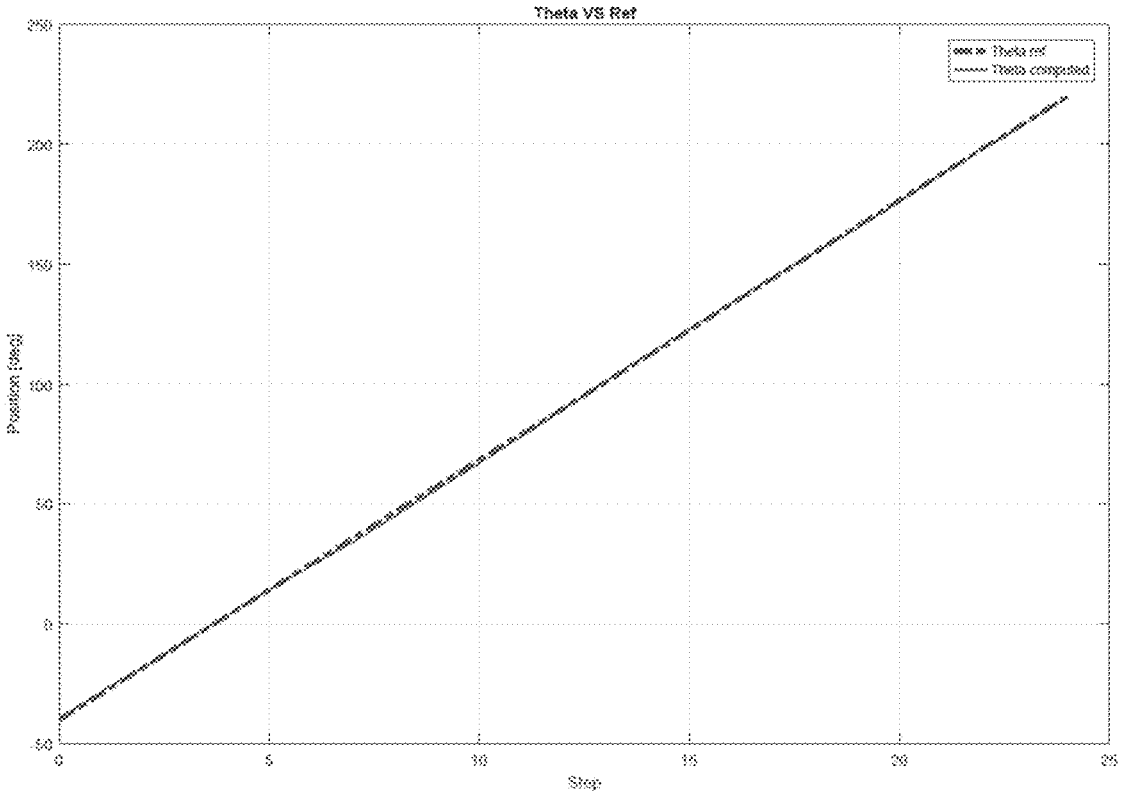

Figure 9E

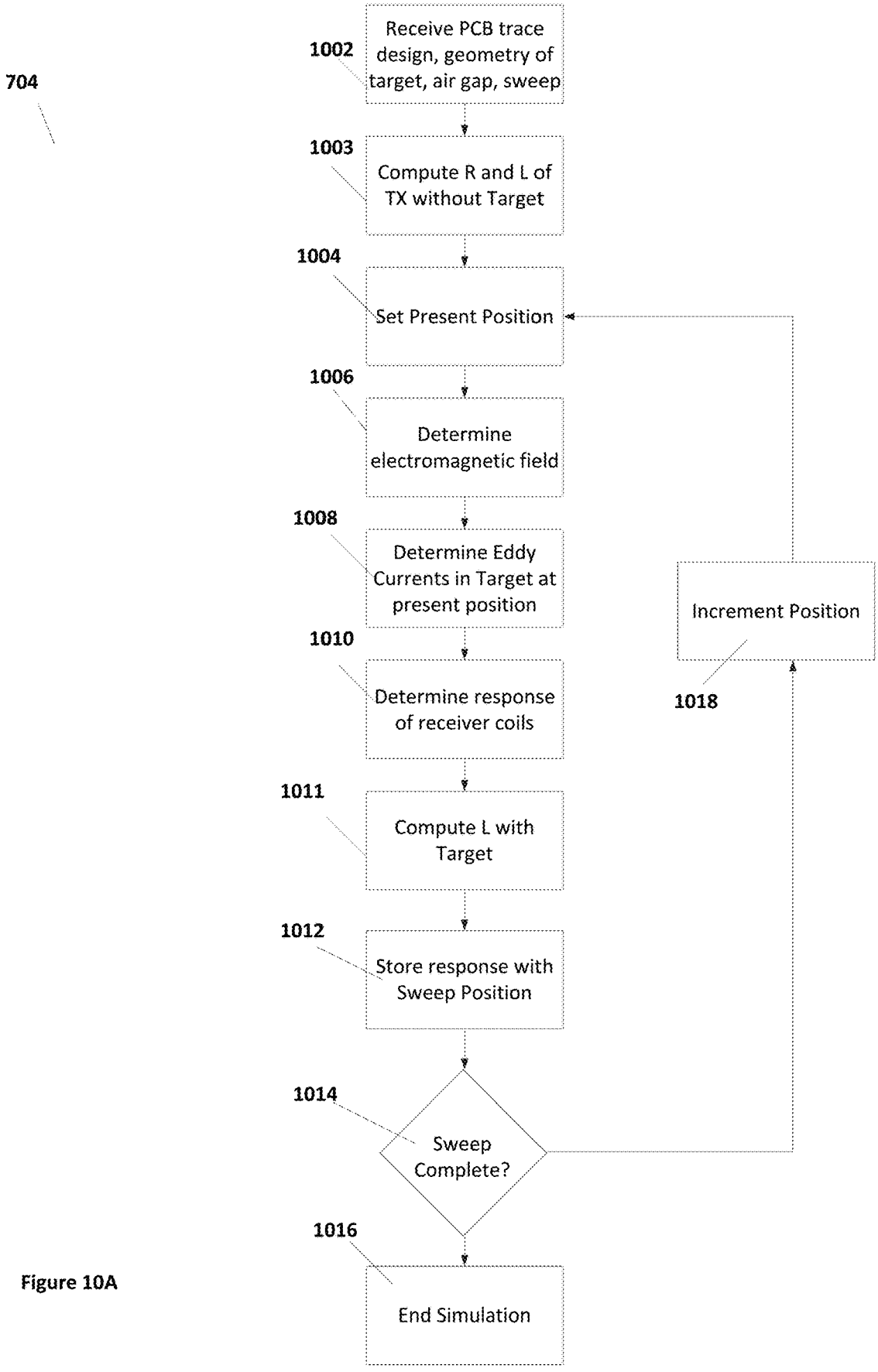
704
1002
Receive PCB trace design, geometry of target, air gap, sweep
1003
Compute R and L of TX without Target
1004
Set Present Position
1006
Determine electromagnetic field
1008
Determine Eddy Currents in Target at present position
1010
Determine response of receiver coils
1011
Compute L with Target
1012
Store response with Sweep Position
1014
Sweep Complete?
1016
End Simulation
Increment Position
1018

Figure 10A

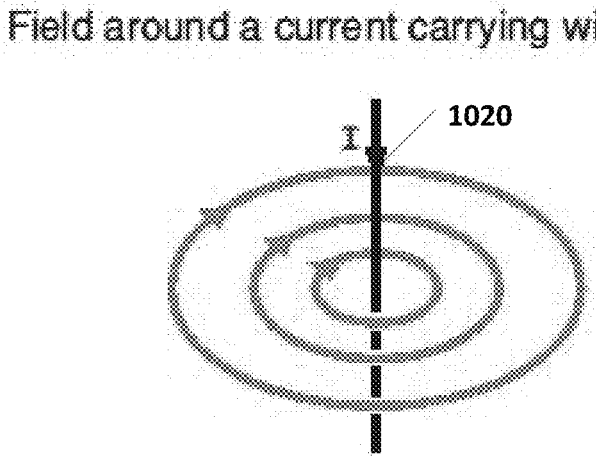

Figure 10B

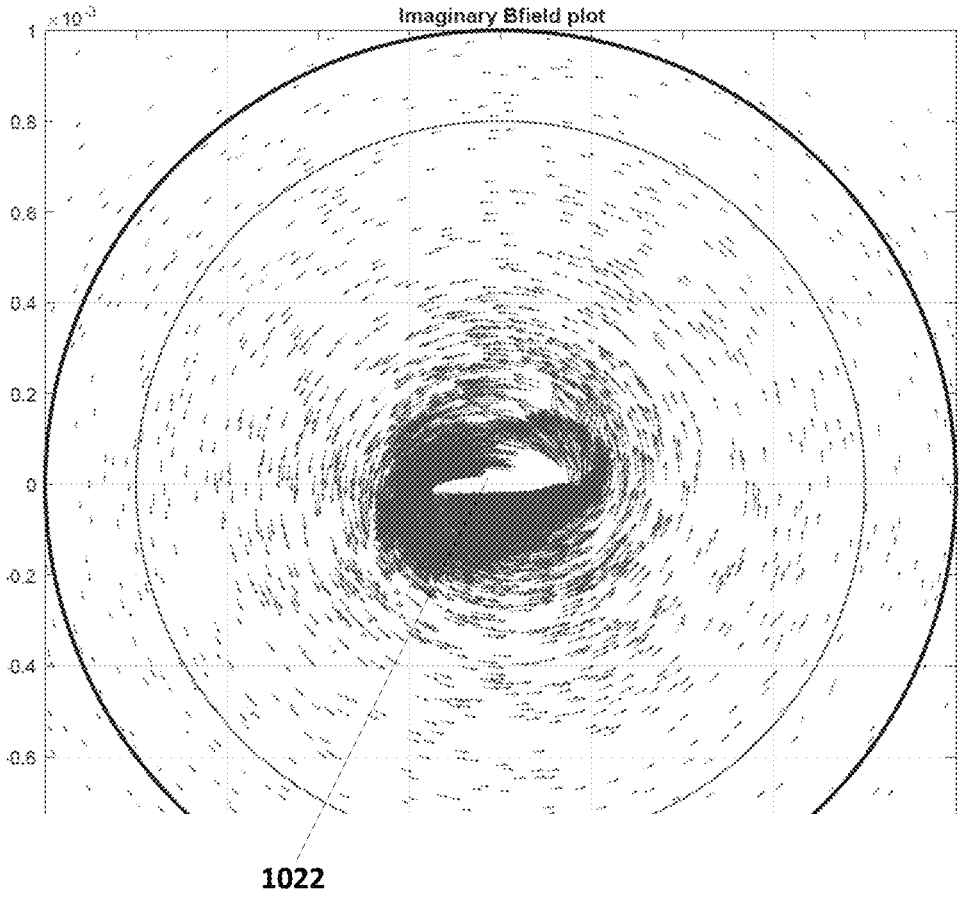

Figure 10C

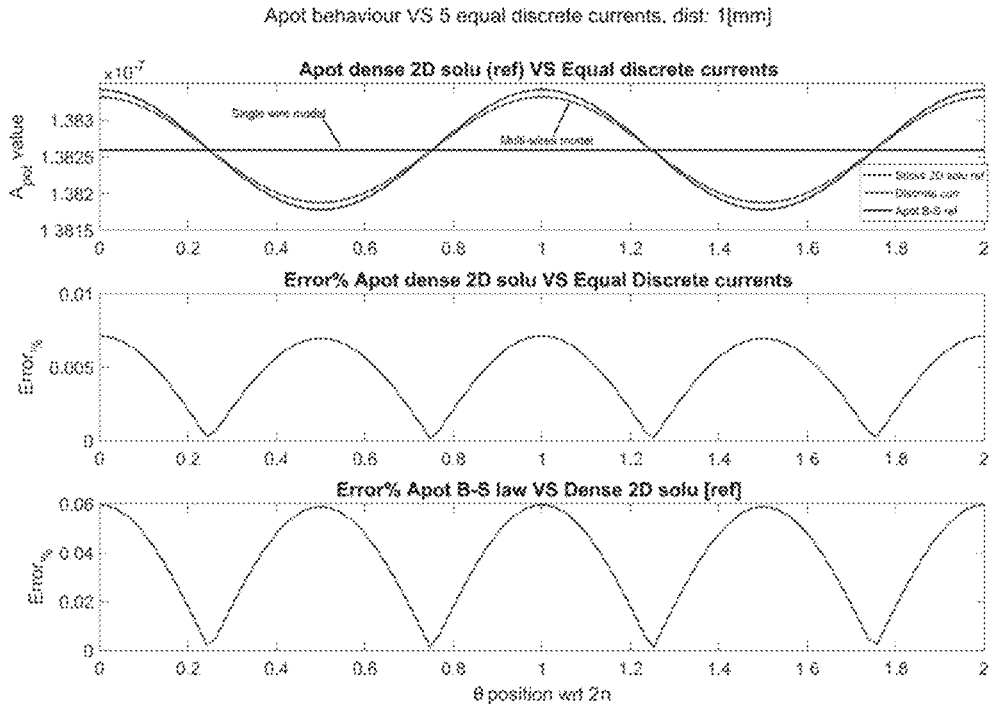

Figure 10D

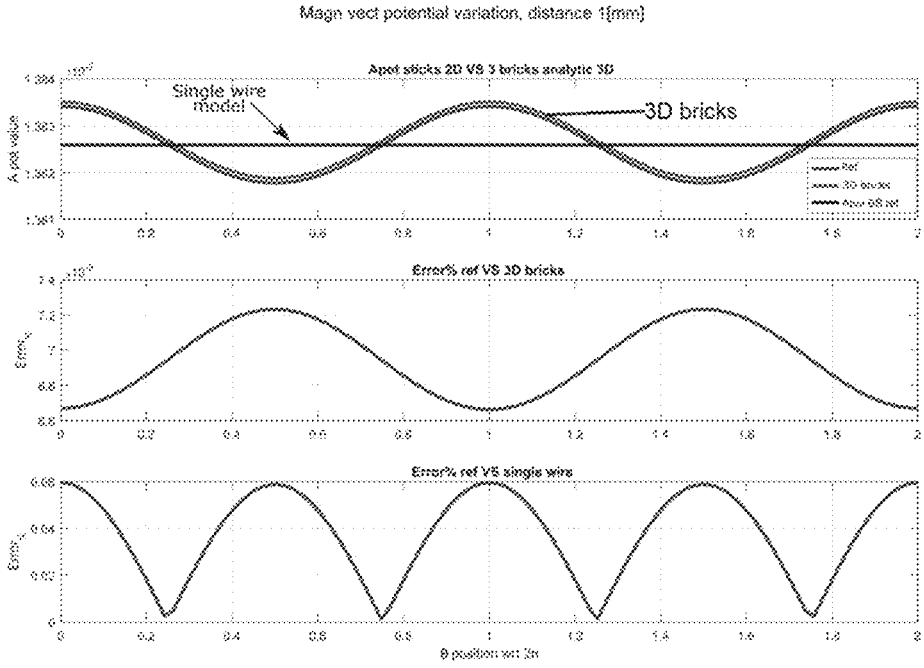

Figure 10E

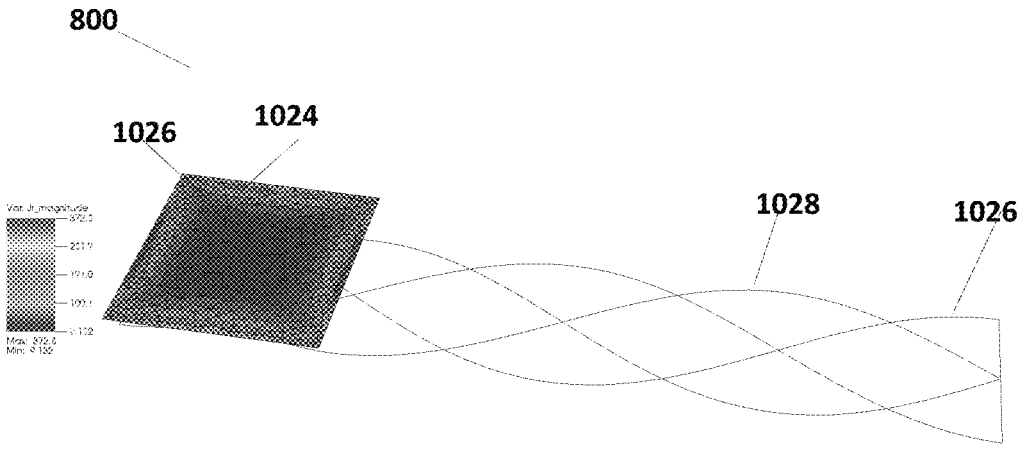

Figure 10F

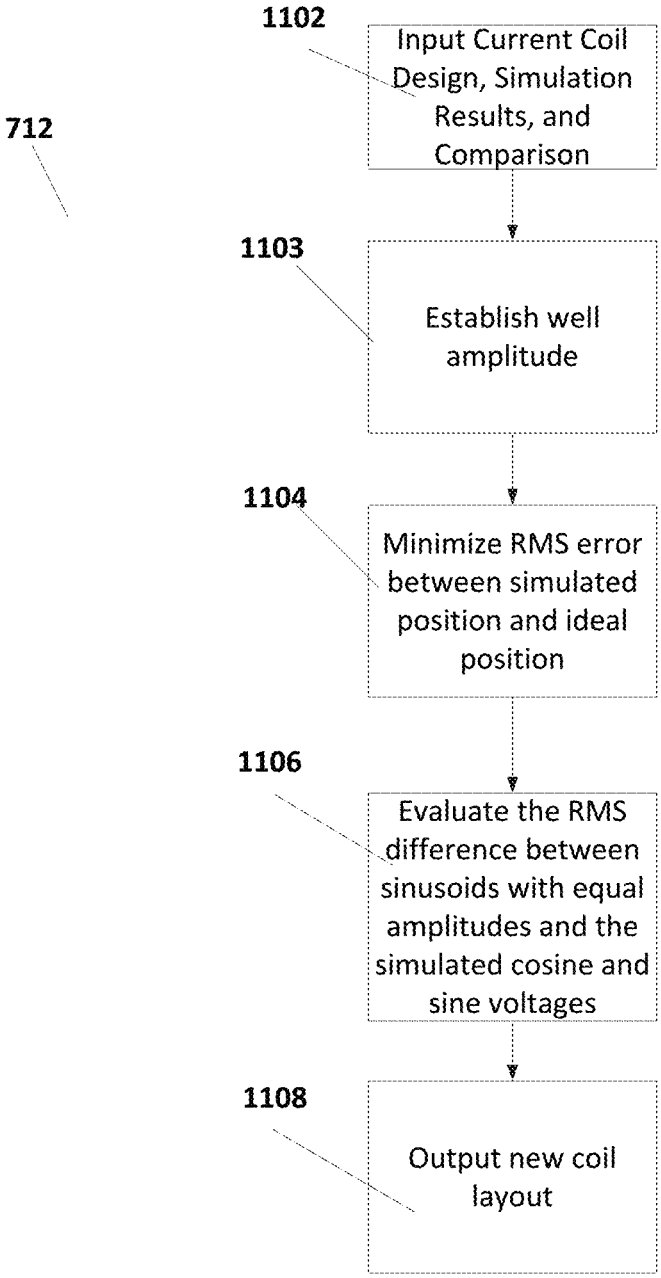
712
1102
Input Current Coil Design, Simulation Results, and Comparison
1103
Establish well amplitude
1104
Minimize RMS error between simulated position and ideal position
1106
Evaluate the RMS difference between sinusoids with equal amplitudes and the simulated cosine and sine voltages
1108
Output new coil layout

Figure 11

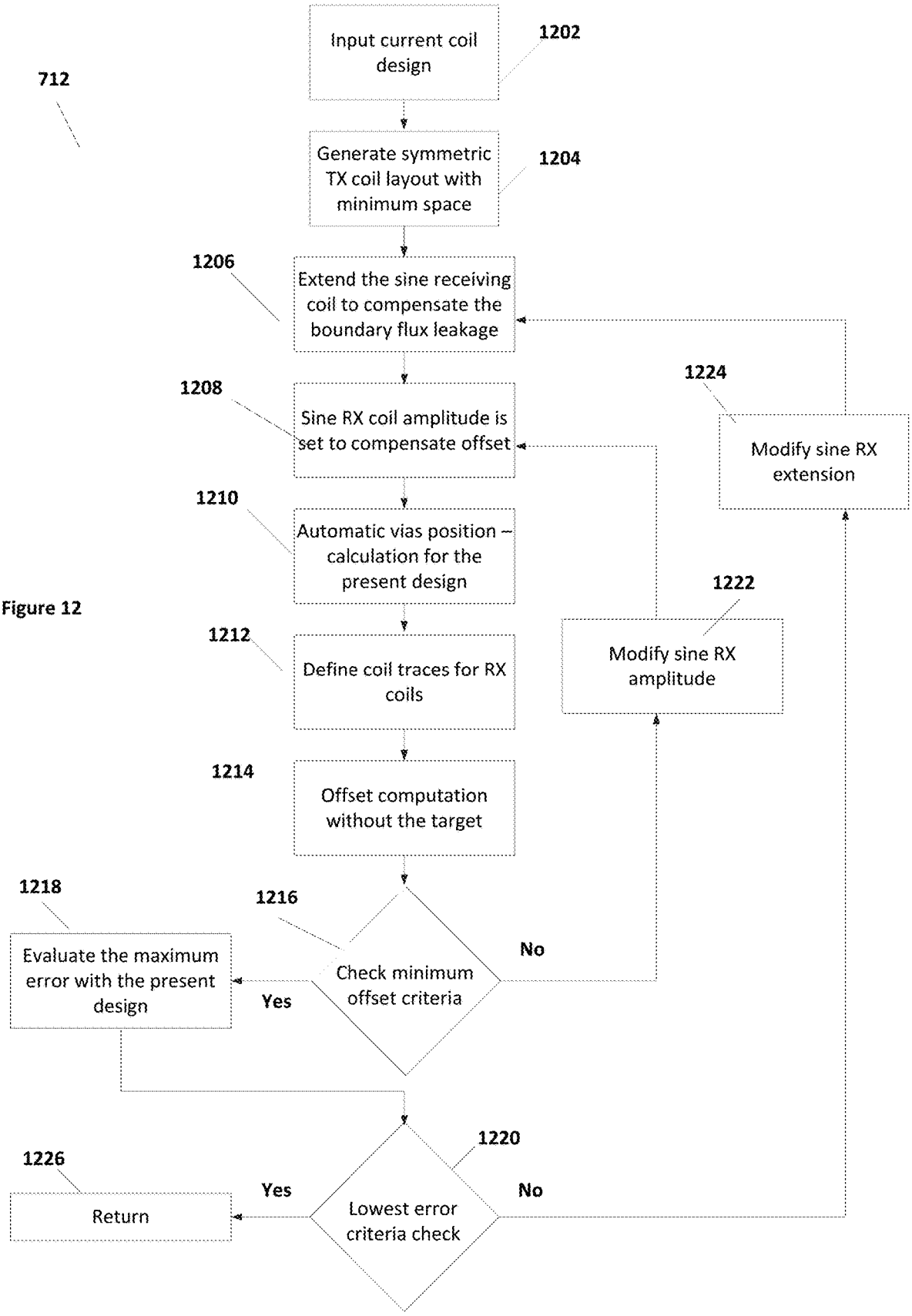
712
Input current coil design
1202
Generate symmetric TX coil layout with minimum space
1204
1206
Extend the sine receiving coil to compensate the boundary flux leakage
1208
Sine RX coil amplitude is set to compensate offset
1224
Modify sine RX extension
1210
Automatic vias position – calculation for the present design
1222
Modify sine RX amplitude
1212
Define coil traces for RX coils
1214
Offset computation without the target
1218
1216
Evaluate the maximum error with the present design
Check minimum offset criteria
No
Yes
1220
1226
Return
Yes
Lowest error criteria check
No

Figure 12

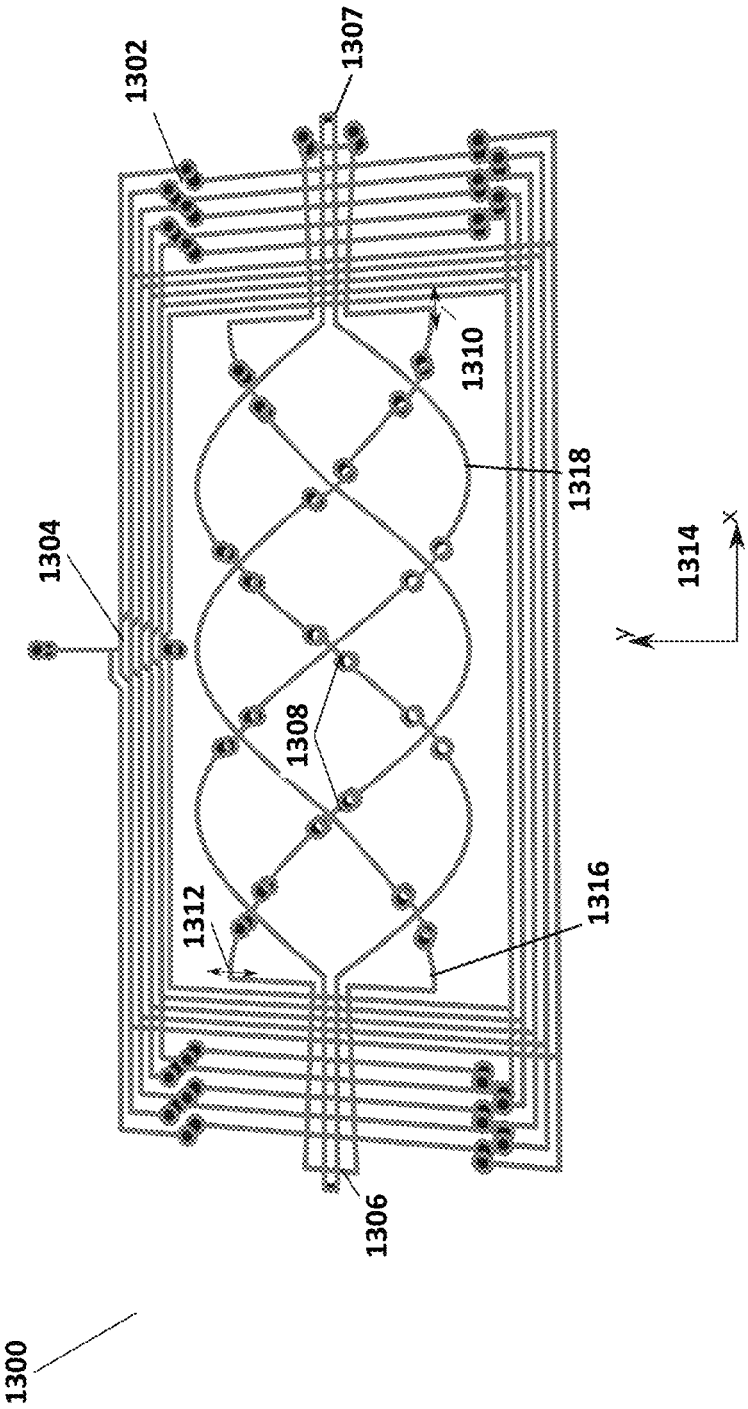

Figures 13

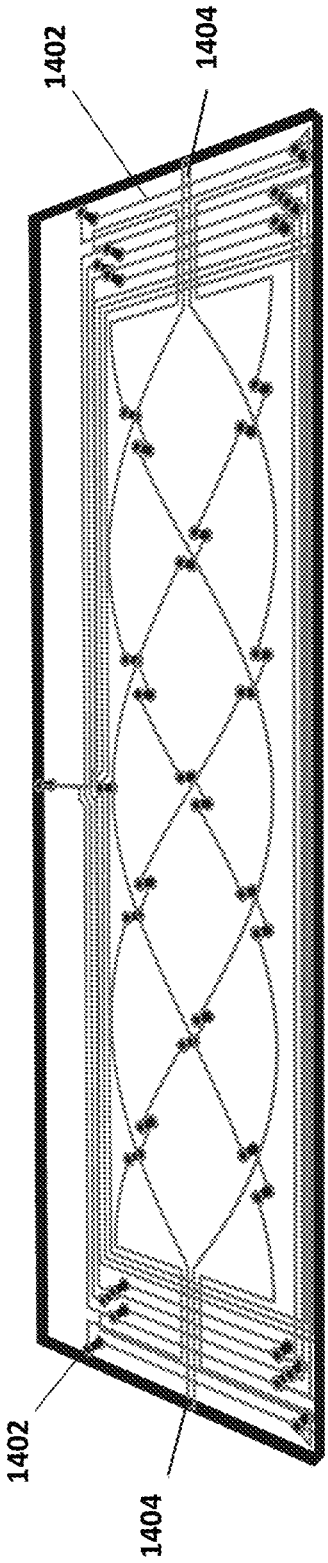

Figure 14

SENSOR COIL OPTIMIZATION

RELATED APPLICATIONS

This disclosure claims priority to U.S. Provisional Application 62/580,354 filed on Nov. 1, 2017, by inventors QAMA and SPECOGNA entitled "Sensor Coil Optimization," which is herein incorporated by reference in its entirety.

TECHNICAL FIELD

Embodiments of the present invention are related to position sensors and, in particular, to optimization of the sensor coils in a position sensor.

DISCUSSION OF RELATED ART

Position sensors are used in various settings for measuring the position of one component with respect to another. Inductive position sensors can be used in automotive, industrial and consumer applications for absolute rotary and linear motion sensing. In many inductive positioning sensing systems, a transmit coil is used to induce eddy currents in a metallic target that is sliding or rotating above a set of receiver coils. Receiver coils receive the magnetic field generated from eddy currents and the transmit coils and provide signals to a processor. The processor uses the signals from the receiver coils to determine the position of the metallic target above the set of coils. The processor, transmitter, and receiver coils may all be formed on a printed circuit board (PCB).

However, these systems exhibit inaccuracies for many reasons. For example, the electromagnetic field generated by the transmitter, and the resulting fields generated in the metallic target, may be non-uniform, the connections of wire traces to the transmit coils and the arrangement of receive coils may result in further non-uniformity. The air-gap (AG) between the metallic target and the coils mounted on the PCB may be non-uniform. Further, the amplitudes of signals generated by receiver coils may have an offset. There may be mismatches between the multiple receiver coils. There may be different coupling effects between the metallic target and each of the multiple receiver coils. These and other factors may result in inaccurate results of the position locating system.

Therefore, there is a need to develop better methods of designing sensor coils that offer better accuracy for position sensing.

SUMMARY

In some embodiments, a coil design system is provided. In particular, a method of providing an optimized position locating sensor coil design in presented. The method includes receiving a coil design; simulating position determination with the coil design to form a simulated performance; comparing the simulated response with the specification to provide a comparison; and modifying the coil design based on a comparison between the simulated performance and a performance specification to arrive at an updated coil design.

These and other embodiments are discussed below with respect to the following figures.

BRIEF DESCRIPTION OF THE FIGURES

FIGS. **1**A and **1**B illustrates a coil system for determining a position of a target.

FIGS. **2**A, **2**B, **2**C, **2**D, and **2**E illustrate response of the receiver coils while sweeping a metallic target across the coil system.

FIGS. **3**A and **3**B illustrate configuration of receive coils on a printed circuit board in a coil system.

FIG. **3**C illustrates inhomogeneity of electromagnetic fields generated by a transmit coil in the coil system.

FIGS. **3**D and **3**E illustrate discrepancies in fields measured by receiver coils in a coil system.

FIG. **4**A illustrates a block diagram of a testing device that tests the accuracy of a position locate system.

FIG. **4**B illustrates a test device such as that illustrated in FIG. **4**A.

FIG. **4**C illustrates testing a position locating system with the test device illustrated in FIG. **4**B.

FIG. **4**D illustrates received voltages from receive coils in the position locating system measured with the test device illustrated in FIG. **4**B.

FIG. **5** illustrates a measured response and a simulated response.

FIG. **6** illustrates an error between the measured and simulated responses of an example coil design optimized according to embodiments of the present invention.

FIGS. **7**A and **7**B illustrate an algorithm for optimizing coil design for a position location sensor according to some embodiments of the present invention.

FIG. **7**C illustrates an input screen shot for a system operating the algorithm illustrated in FIG. **7**A.

FIGS. **8**A and **8**B illustrate a coil design according to some embodiments of the present invention

FIGS. **9**A, **9**B, and **9**C illustrate another example coil design according to some embodiments of the present invention.

FIGS. **9**D and **9**E illustrate performance characteristics of a coil design according to some embodiments.

FIG. **10**A illustrates a simulation algorithm according to some embodiments.

FIGS. **10**B and **10**C illustrate the fields generated around a wire and the fields generated around a rectangular trace.

FIGS. **10**D and **10**E illustrate an error generated by treating a rectangular trace as a one-dimensional wire, multi-wires, or 3D bricks.

FIG. **10**F illustrates a simulation of eddy currents in a metallic target over receiver coils.

FIG. **11** illustrates an algorithm for adjusting the receiver coil design according to some embodiments.

FIG. **12** illustrates another embodiment of an algorithm for adjusting the receiver coil design according to some embodiments.

FIG. **13** illustrates optimizing a design without wells.

FIG. **14** illustrates an optimized design with wells.

These and other aspects of embodiments of the present invention are further discussed below.

DETAILED DESCRIPTION

In the following description, specific details are set forth describing some embodiments of the present invention. It will be apparent, however, to one skilled in the art that some embodiments may be practiced without some or all of these specific details. The specific embodiments disclosed herein are meant to be illustrative but not limiting. One skilled in the art may realize other elements that, although not specifically described here, are within the scope and the spirit of this disclosure.

This description illustrates inventive aspects and embodiments should not be taken as limiting—the claims define the

protected invention. Various changes may be made without departing from the spirit and scope of this description and the claims. In some instances, well-known structures and techniques have not been shown or described in detail in order not to obscure the invention.

FIG. **1**A illustrates a positioning system **100**. As illustrated in FIG. **1**A, the positioning system includes transmit/receive control circuit **102** that is coupled to drive a transmitter coil **106** and receive signals from receive coils **104**. In most configurations, receive coils **104** are located within transmitter coil **106**, however in FIG. **1**A they are illustrated separately for clarification purposes. Receive coils **104** are generally physically located within the border of transmit coil **106**.

Embodiments of the present invention can include a transmitter coil **106**, two receiver coils **104**, and an integrated circuit (IC) **102** driving the transmitter coil **106** and measuring the signals originated in the receiver coils **104** all formed on a printed circuit board (PCB).

FIG. **1**B illustrates a configuration of transmit coils **106** and receive coils **104** in a linear position locating system. As is shown in FIG. **1**B, a conductive metallic target **124** can be positioned over the transmitter coil and the two receiver coils.

As is illustrated in FIG. **1**A, transmit coil **106** is driven to form magnetic field **108**. Transmit coil **106** can be driven at a range of frequencies or at particular frequencies. In FIG. **1**A, magnetic field **108**, with the positive current illustrated by the arrows, is circular around each wire and in a direction that points out of the page inside coil **106** and into the page outside of coil **108** with the current direction as illustrated in FIG. **1**A. Receive coils **104** are located inside coil **106**, as is illustrated in FIG. **1**B. Transmit coil **106** is driven at any frequency that can produce electromagnetic field **108** to induce voltages in receiver coils **104**. In general, there can be any number of receiver coils, however, for ease of discussion, a system with two receiver coils is discussed below.

FIG. **1**B illustrates the arrangement of sensor receive coils (RX) **104** within transmit coil (TX) **106**. As illustrated in FIG. **1**B, sensor receive coils **104** includes a sine wave oriented coil RXSIN **112** and a cosine oriented signal coil RXCOS **110**. Sine wave oriented coil RXSIN **112** includes sine loops **114**, **116**, and **118** where coil **112** is wound in in-phase or anti-phase directions, here depicted as clockwise or counter clockwise depictions, to result in the production of voltages in the loop of opposite sign as a result of the presence of electro-magnetic field **108**. As is illustrated, the wiring of sine wave oriented coil **112** provides a clockwise rotation in loops **114** and **118** resulting in a nominally positive voltage and a counterclockwise rotation in loop **116** resulting in nominally negative voltages. Similarly, cosine oriented coil **110** may include a first loop **120** with a clockwise orientation and a second loop **122** with a counterclockwise orientation FIG. **1**B illustrates a possible electromotive force reference direction, as indicated by the arrows, that is consistent with the magnetic fields produced by transmitter coil **106** as illustrated in FIG. **1**A. As one skilled in the art will recognize, the orientations may be interpreted otherwise.

In the system illustrated in FIG. **1**B, the transmitter coil (TX) **106** is stimulated by the circuit **102**, which may be an integrated circuit, to generate a variable Electromagnetic field (EMF), illustrated as EMF field **108**. The magnetic field **108** couples with the receiver coils (RX) **104**. If a conductive metallic target **124** is placed on the top of the receiver coils **104** as illustrated in FIG. **1**B, an eddy current is generated in the metallic target **124**. This eddy current generates a new electromagnetic field that is ideally equal and opposite of field **108**, canceling the field in receiver coils **104** directly under metallic target **124**. The receiver coils (RX) **104** capture the variable EMF field **108** generated by the transmit coils **106** and those induced by metallic target **124**, resulting in sinusoidal voltages generated at the terminals of receiver coils **104**.

In absence of metallic target **124**, there will be no voltage at the terminals of the RX coils **104** (labeled RxCOS **110** and RXSin **112** in FIG. **1**B). When metallic target **124** is placed in a specific position with respect to the RX coils **104**, the resultant electromagnetic field on the area covered by the metallic target **124** is ideally zero and therefore the voltages at the terminals of the RX coils **104** will have different characteristic depending on the location of metallic target **124** relative to receiver coils **104**. The RX coils **104** are designed in a way that a sine voltage is created at the terminals of one RX coil (RxSin **112**) and a cosine voltage is created at the terminals of the other RX coil (RxCos **110**) as metallic target **124** is swept across receiver coils **104**. The position of the target with respect to the RX coils **104** modulates the amplitude and the phase of the voltage at the terminals of the RX coils **104**.

As illustrated in FIG. **1**A and discussed above, transmitter coil **106**, receive coils **104**, and transmit/receive circuit **102** can be mounted on a single PCB. Further, the PCB can be positioned such that metallic target **124** is positioned above receive coils **104** and spaced from receive coils **104** by a particular spacing, the air gap (AG). The position of metallic target **124** relative to the PCB on which receive coils **104** and transmitter coil **106** is mounted can be determined by processing the signals generated by sine oriented coil **112** and cosine oriented coil **110**. Below, the determination of the position of metallic target **124** with respect to receive coils **104** is described in a theoretical ideal condition.

In FIG. **1**B, metallic target **124** is located at a first location. In this example, FIG. **1**B and FIGS. **2**A, **2**B, and **2**C depict operation of a linear position locator system. The principle of operation is the same in both linear and circular locators. In the discussion below, the position is given in relation to the construction of cosine oriented coil **110** and sine oriented coil **112** by providing the angular relations with respect to the sine operation of sine oriented coil **112** which results from the position of the leading edge of metallic target **124** and coils **110** and **112**. The actual position of metallic target **124** in such a system can be derived from the angular position as measured by the output voltages of receive coils **104** and the topology of receive coils **110** and **112**. Furthermore, as illustrated in FIG. **1**B, the topology of coil **110** and the topology of coil **112** are coordinated to provide indication of the location of metallic target **124**.

FIG. **2**A illustrates the 0° position of metallic target **124** with cosine oriented coil **110** and sine oriented coil **112** separated for ease of explanation. As shown in FIG. **1**B, sine oriented coil **112** and cosine oriented coil **110** are co-located within transmit coil **106**. Using the magnetic field **108** as illustrated in FIG. **1**A, loops **114**, **116**, and **118** of sine oriented coil **112** are positioned such that the sum of the voltages in each loop cancels so that the total V_{sin} is 0. As illustrated in FIG. **2**A, in the absence of metallic target **124**, the voltage in loop **114**, V_c can be represented as ½, the voltage in loop **116** (because the current in that loop is opposite the current in loops **114** and **118**) can be represented as V_d=−1, and the voltage in loop **118** can be represented as V_e=½. Consequently, the voltage in coil **112** is V_{sin}=V_c+

$V_d+V_e=0$. Consequently, if metallic target **124** is not present, then the output signal from sine oriented coil **112** would be 0.

Similarly, if metallic target **124** is not present, then the output signal from cosine oriented loop **110** is also 0 because the voltage generated by magnetic field **108** in loop **120**, $V_a=-1$ cancels the voltage generated by magnetic field **108** in loop **122**, $V_b=1$, so that $V_{cos}=V_a+V_b=0$. As discussed above, the voltage depictions provided here are proportional and depicted as a proportion of a full loop—loops **120**, **122**, and **116** can have a maximum representation of 1 while loops **114** and **118** can have a maximum representation of ½. The sign represents the reference direction of the loop, which results in generation of the voltage from that loop. The reference direction is arbitrary and consistent results can be calculated regardless of which of the two possible directions is chosen to depict positive.

However, with metallic target **124** placed at the 0° position, the magnetic field **108** in loop **114** of sine oriented coil **112** is canceled by eddy currents generated in metallic target **124** so that $V_c=0$. In loop **116** of sine oriented coil **112**, the magnetic field **108** in the half of loop **116** under metallic target **124** is canceled by eddy currents formed in metallic target **124**, but a voltage is generated by the magnetic field **108** in the half of loop **116** that does not lie under metallic target **124**. Since half of loop **116** is exposed, the voltage generated is $V_d=-½$. Further, voltage is generated in loop **118** of sine oriented coil **112** such that V_e is ½. However, the voltage generated by loop **116** is canceled by the voltage generated in loop **118**, resulting in the voltage signal across sine oriented loop **112** is 0; $V_{sin}=V_c+V_d+V_e=0$.

In the same orientation of metallic target **124** with respect to cosine oriented coil **110**, loop **120** is covered by metallic target **124** so that $V_a=0$. Loop **122** is exposed so that $V_b=1$. Therefore, the voltage across cosine oriented coil **110**, V_{cos}, is given by $V_a+V_b=1$.

FIG. **2**B illustrates metallic target **124** in a 90° position with respect to sine oriented coil **112** and cosine oriented coil **110**. As illustrated in FIG. **2**B, in sine oriented coil **112**, metallic target **124** covers completely loop **116** and leaves loops **114** and **118** uncovered. As a consequence, $V_c=½$, $V_d=0$, and $V_e=½$ so that $V_{sin}=V_c+V_d+V_e=1$. Similarly, in cosine oriented coil **110**, half of loop **120** is covered resulting in $V_a=-½$ and half of loop **122** is covered resulting in $V_b=½$. Consequently, V_{cos}, given by V_a+V_b, is 0.

Similarly, FIG. **2**C illustrates metallic target **124** in a 180° position with respect to sine oriented coil **112** and cosine oriented coil **110**. Consequently, half of loop **116** and loop **118** in sine oriented coil **112** are covered by metallic target **124** and loop **122** in cosine oriented loop **110** is covered by metallic target **124**. Therefore $V_a=-1$, $V_b=0$, $V_c=½$, $V_d=-½$, and $V_e=0$. As a result, $V_{sin}=0$ and $V_{cos}=-1$.

FIG. **2**D illustrates a graph of V_{cos} and V_{sin} versus angular position of metallic target **124** with the coil topology provided in FIGS. **2**A, **2**B, and **2**C. As is illustrated in FIG. **2**D, the angular position can be determined by processing the values of V_{cos} and V_{sin}. As illustrated by sweeping the target from a defined initial position to a defined end position, in the output of the receivers will be generated a sinusoidal (V sin) and cosinusoidal (V cos) voltage illustrated in FIG. **2**D.

The angular position of metallic target **124** relative to receive coils **104** can be determined from the values of V sin from sine oriented coil **112** and V cos cosine oriented coil **110** as is illustrated in FIG. **2**E. For example, the angular position of the target can be calculated as

$$\text{Angular position}=\arctan(V\sin/V\cos).$$

FIG. **2**E illustrates this and shows the sinusoidal forms of V_{cos} and V_{sin} along with the determination of the position of metallic target **124** derived from the values of V_{cos} and V_{sin}. In a linear position locating system, the linear position can be determined by the angular position through knowledge of the wavelength of the sinusoidal forms of the traces of receiver coils **104** (i.e., the separation between peak separation areas of the traces of the sine oriented coil **112** and the cosine oriented coil **110**). In an angular position locating system, the sine oriented coil **112** and cosine oriented coil **110** can be arranged such that the angular position can be equal to the actual angular position of the metallic target **124** with respect to the rotation of metallic target **124**.

It is important to note the following conditions that indicate an ideal operation of position location sensor **100**. Among those conditions are that the shape of transmitter coil **106** has no importance as long as it covers the area where the receiver coils **104** are placed. Further, the shape of the receiver coils **104** is equal to a perfect geometrical overlapped sine and cosine. Additionally, the shape of metallic target **124** has no influence on the working principle as long as the area of the target covers a part of the total area of the receiver coils **104**.

These conditions for an ideal set of coils and ideal metallic target are never met. In a real system, the situation is very different. The non-ideality leads to inaccuracy in the determination of the position of metallic target **124**. Among the issues that result in inaccuracies in location determination include non-uniformity of the electromagnetic field generated in transmit coil **106**; connections of metallic traces between transmit/receive circuit **102** and receive coils **104** and connections of metallic traces between transmit/receive circuit **102** and transmit coil **106**, which also contribute to the generated electromagnetic fields; the air gap (AG) between metallic target **124** and the PCB on which receive coils **104** and transmit coil **106** is mounted; amplitude offsets between sine oriented coils **112** and cosine oriented coils **110**; mismatches between signals from receive sine oriented coils **112** and cosine oriented coils **110**; different coupling effects in sine oriented coils **112** and cosine oriented coils **110**. Further, there is a strong correlation between the air gap (AG) between the metallic target **124** and the PCB and the accuracy of the location determination. Furthermore, in the ideal world, the topology of sine oriented coil **112** and cosine oriented coil **110** are ideal trigonometric functions but in an actual design these coils **104** are not ideal and have several through vias to allow traces to be intertwined on the PCB by using both sides of the PCB.

FIG. **3**A illustrates a sine oriented coil **112** oriented on a PCB (not shown in FIG. **3**A for clarity). The PCB is positioned such that traces that form sine oriented coil **112** are positioned on a top side and a bottom side of the PCB. In this disclosure, references to the top side or the bottom side of the PCB indicated opposite side of the PCB and have no other meaning regarding the orientation of the PCB. In general, the position locating system is oriented such that the top side of the PCB faces a surface of metallic target **124**. FIG. **3**B illustrates a top side of PCB **322** on which top side traces for formation of transmit coil **106**, sine oriented receiver coil **112**, and cosine oriented receiver coil **110** are formed.

As is illustrated in FIG. **3**A, coil **112** is formed by traces **302** on the top side of the PCB **322** and traces **304** on the bottom side of the PCB **322**. Traces **302** and **304** are electrically joined by vias **306** formed through the PCB **322**. As is illustrated in FIG. **3**A, vias **306**, top side traces **302**, and bottom side traces **304** are arranged to allow formation

of cosine oriented coil **112**. For example, portions **310** and **312** allow for crossing of coil **112** to form loops **114**, **116**, and **118** while separated the traces at the intersection. As is further illustrated, portions **314**, **316**, **318**, and **320** allow for overlay of cosine oriented coil **112** on the PCB.

However, vias **306** and the existence of traces **302** and **304** on opposite sides of PCB **322** decrease the effective amplitude of the signal detected by coils **104**. Effectively, vias **306** make the gap distance between transmit coil **106** and signal coils **104**, which has a large influence in itself on accuracy of the position locating system. This is combined with the increase in the effective air gap between metallic target **124** and signal coils **104** on the PCB **322** due to traces of signal coils **104** being formed both on the top side and the bottom side of PCB **322**.

FIG. **3**B illustrates a further problem with symmetries where transmit coil **106** is not symmetric with receive coils **104**. In the case shown in FIG. **3**B, receive coils **104** are not centered on the transmit coils **106** and the traces that form connections to receive coils **104** and to transmit coil **106** are also not symmetric.

FIG. **3**C illustrates the non-uniformity of the magnetic field strength generated by transmit coils **106**. As is illustrated in FIG. **3**C, two traces of transmit coil **106** are located at positions 0 and 5 on the graph while receive coils **104** are positioned between positions 0 and 5. FIG. **3**C illustrates the magnetic field between these traces has a minimum between the two traces. FIG. **3**C does not illustrate the further distortion because of the two traces that connect the two traces illustrated in FIG. **3**C and run perpendicular to the traces illustrated in FIG. **3**C.

FIG. **3**D and FIG. **3**E further illustrates inaccuracies that can result from displacements in transmit coil **106**. As illustrated in FIGS. **3**D and **3**E, transmit coil **106** includes a displacement **330** that distorts the magnetic field produced by transmit coil **106**. Stray fields from displacement **330** produce imbalances in the receive coils **104**. Consequently, inaccuracies in position determination will develop from such features.

FIGS. **4**A and **4**B illustrate a calibration and test device **400** that can be used to evaluate position locating systems. Due to non-idealities of the magnetic coupling principle such as those described above, a calibration procedure can be used to correct the measured position of the target with respect to the positioning device. Furthermore, system **400** can be used to test the accuracy of positioning systems such as those described above.

FIG. **4**A illustrates a block diagram of an example system **400**. As is illustrated in FIG. **4**A, a metallic target **408** is mounted on a platform **406** such that is over a position locating system **410**. A positioner **404** is capable of moving platform **406** relative to position locating system **410** in a precise manner. As discussed above, position locating system **410** includes transmit coils and receive coils formed on a PCB and may include a controller **402** that receives and processes signals from the receive coils and drives the transmit coil.

As is further shown in FIG. **4**A, metallic target **408** is positioning in a z-direction to provide an air gap (AG) between metallic target **408** and position locating system **410**. In some embodiments, positioner **404** is capable of moving metallic target **408** linearly in an x-y plane as illustrated in coordinate system **420**. In some embodiments, positioner **404** rotates metallic target **408** around a center-of-rotation over position locator system **410** as needed, for example, for testing a rotation locator rather than a linear locator.

Controller **402** is coupled to provide control signals and receive the receive coil signals from positioner **404**. Controller **402** is further coupled to provide transmit power to transmit coils on locating system **410** and to receive and process signals from receive coils in locating system **410**. As illustrated above, position locating system **410** may include a transmit coil **106**, cosine oriented coil **110**, and sine oriented coil **112** as discussed above. In some cases, controller **402** may be mounted on the same PCB with transmit coil **106**, cosine oriented coil **110**, and sine oriented coil **112** of locating system **410** and provide locate signals to a separate processor **422**.

Processor **422** can be any processing system capable of interfacing to controller **402** and to positioner **404**. As such, processor **422** may include one or more microcomputers, transient and nontransient memory, and interfaces. Processor **404** communicates with positioner to determine the precise location of metallic target **408** with respect to position locating system **410** and to provide signals to positioner **404** that determine the sweep of metallic target **408** over the receive coils mounted in position locating system **410**. As such, processing unit **422** can compare the measured position of metallic target **408** as determined by controller **402** with the determined position as provided by positioner **404** to evaluate the accuracy of position locating system **410**. In some embodiments, controller **402** may be combined with processing unit **422**, which performs all of the tasks for determining the actual position of metallic target **408** from positioner **404** and the measured position of metallic target **408** from coils on position locating system **410** and determining the accuracy of the measured position from position locating system **410**.

As is further illustrated in FIG. **4**A, controller **402** can include a processor **412** (which may a processor in processor **422**) that drives the transmit coils through driver **414** and receives signals from the receive coils as well as processes the data from the receive coils in order to determine the location of metallic target **508** relative to the receive coils. Processor **412** can, through interface **424**, communicate with devices such as processing unit **422**. Further, processor **412** drives a transmit coil such as transmit coil **106** through a driver **404**. Driver **404** may include circuitry such as digital-to-analog converters and amplifiers to provide current to transmit coils such as transmit coil **106**. Additionally, processor **412** can receive the receive signals V sin and V cos from receive coils such as coils **110** and **112**. The signals V sin and V cos from the receive coils is received into buffers **416** and **418**, which may include circuitry such as filters and amplifiers as well as analog-to-digital converters to provide digital data to processor **412**. Processor **412** can calculate a position as described above to provide positional data of metallic target **408** with respect to the receive coils on position locating system **410**.

FIG. **4**B illustrates an example of positioning system **400**. Positioner **404** is coupled to a mount **406** and can include four stepper motors that provide a 4-axis movement of the target—x, y, z and rotational around the z axis. As such, system **400** as illustrated in FIG. **4**B is able to sweep the metallic target **408** on the top of the receiver coils in position locator system **410** in all possible directions, including the z direction to create different air gaps. As discussed before, the air gap is the distance between the metallic target **408** and the PCB where the transmit and receive coils of position locate system **410** are placed. Such a system can be used for calibration, linearization, and analyzing the accuracy of position locator system **410**.

FIG. **4**C illustrates a sweep of a metallic target **408** over a rotation position locator system **410** with transmit coils **106** and receive coils **104**. As is illustrated in FIG. **4**C, metallic target **408** is swept from 0° to θ° over receiver coils **104**. FIG. **4**D illustrates an example of the voltages V sin and V cos measured from receiver coils **104** compared with the results of the simulation as metallic target **408** is swept as illustrated in FIG. **4**C. In the particular example of FIG. **4**D, metallic target **408** is swept in 50 positions. The crosses represent the sample voltages and the continuous lines represents values simulated by an electromagnetic field solver program, CDICE-BIM.

The accuracy of position locator system **410** can be defined as the difference between the measurement of the position during a sweep of the metallic target **408** from an initial position to an end position and an expected ideal curve for that sweep. This result is expressed in percentage respect to the full scale, as is illustrated in FIG. **5**. In FIG. **5**, Pos0 is the measured value from position locating system **410** and the output-fit is the ideal curve.

$$FNL = \frac{100(Pos0 - \text{Ideal}_{curve})}{Fs}$$

Pos0 is the value measured from a register of controller **402** while FS is the value at full scale. For example, with a 16 bit register FS is 2E16−1=65535. FIG. **6** illustrates the error in terms of FNL % FS as determined by the above equation. The goal is to produce position sensing with the best possible accuracy, for example of 0.2% FS or less.

If the coil design on a PCB is designed using a trial and error method, the best achieved accuracy is 2.5% FS-3% FS. In a sensor formed on a PCB there are two receiver coils and one transmitter coil. The accuracy of the position measured is extremely relevant to the coil design. Trial and error coil design on PCB have empirically attempted to resolves these issues. However, such a simplified and inaccurate method can only take into account a limited set of the issues. All these procedures do not lead to a successful design because the whole system, coil—target—traces, is more complex than can be easily accounted for and the optimal solution has to take into account a more substantial number of the parameters if the resulting coil design will meet desired accuracy specifications.

FIG. **7**A illustrates an algorithm **700** for providing a coil design on a printed circuit board for an accurate position locating system according to some embodiments of the present invention. Algorithm **700** can be executed on a computing system with sufficient computing power to execute the appropriate simulations. Such a system would typically include a processor coupled to memory. The memory may include both volatile and non-volatile memory for storage of data and programming. In some cases, fixed storage such as hard drives and such can be utilized. The system would include user interfaces such as keyboards, touchscreens, video displays, pointing devices, or other common components. The system would be capable of executing the algorithms described here, interacting with a user, and outputting a finalized coil design for production of a printed circuit board with the optimized design.

As illustrated in FIG. **7**A, algorithm **700** starts with an input step **702**. In step **702**, a first coil design is input for optimization. In particular, the coordinates, layout, and characteristics of the transmit coil and the receive coils are entered, including information regarding connection nodes, vias, and other parameters regarding these coils. Additionally, the design of the metallic target, including the air gap distance between the metallic target and the coils, is input. Further, the desired specification for the accuracy of the position location system that results is provided. System operating parameters (e.g., the frequency and strength at which transmit coils are expected to be driven) are also input. Once the data is input to algorithm **700** in step **702**, algorithm **700** continues to step **704**. FIG. **7**C illustrates a screen-shot indicating input of coil design parameters of step **702**.

In step **704**, the response to the input of power to the transmit coil with the metallic target at various position through its sweep is simulated. In particular, the fields generated by the metallic target in response to the fields generated by the transmit coil is determined. From those fields, the response of the receive coils for the current coil design is simulated. From the receive coil response, a position of the metallic target calculated from the receive coil response is compared with the position of the metallic target as set during the simulation.

In step **706**, the simulated position is compared to the set position position of the metallic target. In step **708**, if the specification is met, algorithm **700** proceeds to step **710** where the final optimized coil design is output. In step **708**, if the specification is not met algorithm **700** proceeds to step **712**.

In step **712**, the design of the coils on the PCB are adjusted in accordance with simulated results from step **704** and the comparison in step **706** in order to improve the accuracy of the finally designed coil design. In some embodiment, the transmitter coil design remains fixed as input into step **702** and the receiver coil design and layout are adjusted to improve accuracy. In some embodiments, the transmitter coil may also be adjusted to improve accuracy.

Algorithm **700** shown in FIG. **7**A results in a coil design for printing on a printed circuit board with a simulated accuracy as specified during the specification input that occurred in step **702**. FIG. **7**B illustrates an algorithm **720** for verifying a coil design, which may be the coil design produced by algorithm **700** in FIG. **7**A.

As shown in FIG. **7**B, a coil design is input in step **722**. The coil design may be an older legacy design, may be a new design, or may have been produced by algorithm **700** as illustrated in FIG. **7**A. In step **724**, a simulation is performed on the coil design. In some cases, where the coil design input is produced by algorithm **700**, this simulation has already been performed in step **704** of algorithm **700**. Otherwise, a similar simulation is performed. In step **726**, the coil design is physically produced on a printed circuit board. In step **728**, the physically produced coil design response is measured, for example with positioning system **400** as illustrated in FIGS. **4**A and **4**B.

In step **730**, the measured results from the physically produced coil design are compared with the simulated results from the coil design. Step **730** may, then, validate the simulation performed in step **724** with respect to its accuracy. In step **732**, if the simulation matches the measured results, then algorithm **720** proceeds to step **734** where the coil design has been validated. In step **732**, if the simulated results do not match the physically measured results, then algorithm **720** proceeds to step **736**.

In step **736**, if algorithm **720** is being performed as a validation of a coil design produced by algorithm **700**, the input design to algorithm **700** is modified and algorithm **700** rerun. In some embodiments, in step **736** an error is produced indicating that the simulation is not operating prop-

erly and therefore the simulation itself need adjusting in order to better simulate all of the non-idealities in the particular position locating system. In that case, step **736** can also be a model calibration algorithm.

Consequently, in some embodiments of the present invention, an optimized coil design can be produced by iteratively providing a simulation of the current coil design and then modifying the coil design according to the simulation until the coil design meets specifications as desired. In some cases, as a final step, the optimized coil design is physically produced and tested to insure that the simulation matches the physically measured properties. This procedure can help to optimize the coil design, whether the goal is to optimize and redesign an old coil design on PCB or whether the goal is to design and optimize a new coil design on PCB.

An existing coil design on a PCB can be validated according to algorithm **720** and potentially improved according to algorithm **700**. The existing coil design can be extracted, for example, in a Gerber format using electronic design automation (EDA) or computer-aided design (CAD) systems. In some embodiments, inputs of the initial coil design in step **702** of Algorithm **700** or step **722** in algorithm **720** can be performed in the Gerber format. The output design in step **710** can also be in the Gerber format. Gerber formatting is commonly used in CAD/CAM systems and the such for representing printed circuit board design and can be obtained from Ucamco USA, San Francisco, Calif.

As such, an existing design can be extracted from the existing printed circuit board and provided to algorithm **720** in step **722** for validation or to algorithm **700** in step **702**. As such, as described above, the performance of the existing design can be performed in step **724** and the actual performance measured in step **728**. The simulated and measured responses can be compared in step **730** and the system validated in step **732**.

As discussed above, measuring the response in step **728** can include sweeping the metallic target from a start point to an end point with constant air gap. The simulation can be run with the same PCB design with the same Air Gap and with the same target. This process, called a validation processes, is important to understand if the simulation is performing correctly and the simulation reflects all the non-ideality present in the design.

Once the capability to simulate correctly the coils on the PCB has been validated, then existing design can be input to step **702** of algorithm **700** and modified in a way to improve the accuracy, for example the offset and nonlinearity, of the resulting position locating system. This approach can be accomplished automatically in the iterative algorithm illustrated by steps **704**, **706**, **708** and **712** of FIG. **7**A and uses a simulation code in step **704** and a coil design code in step **712** to converge on an optimum design. The improved Design Coil, which is output in step **710**, can then be printed on a PCB with the help of an EDA Tool.

A completely new design can be implemented in much the same way that an existing design can be implemented. In particular, the new design can be input to step **702** of algorithm **700** and algorithm **700** can be executed to optimize the coil design. The optimized coil design output in step **710** of algorithm **700** can then be input to algorithm **720** and the design actually produced for testing. Algorithm **720** can then validate operation of the optimized coil design, as discussed above

The coil design tool executed in step **712** of algorithm **700** can be used to design the geometrical shape of the sine and cosine on a PCB using the coil design tool of step **712** in accordance with the simulations performed by simulation tools in step **704**. The iterative algorithm for optimizing the coil design, as illustrated in algorithm **700**, includes the simulation tool in step **704** and the coil design tool of step **712**. In particular, algorithm **700** calculates the minimum position error in step **706** and minimizes non idealities of the Rx Coils in steps **706**, **708** and **712**. With the coordinates obtained after this optimization, PCB can be printed using a commercial EDA tool as in step **710**.

Embodiments of the invention can be used to produce coil designs for position locating systems for all the applications that need position sensor technology, torque, torque angle sensors (TAS) and every other application that uses inductive principle and receiver coils on a PCB. The benefits of certain embodiments include having zero offset on both receivers, which means achieving the theoretic limit that is zero. Achieving 0.5% FS error from a starting point of 2.5% FS-3% FS that occurred before the optimized Coil (an improvement of a factor of 6) can be achieved. Further, no linearization or calibration method is needed if the error is reduced well enough. Additionally, the number of trials and errors used to produce a viable coil design can be reduced, providing for a shortened product introduction and time to market.

FIGS. **8**A and **8**B illustrate an example of a coil layout **800** on a PCB (not shown for clarity) that can be used as an input to algorithm **700** as illustrated in FIG. **7**A. In some cases, the optimized coil design resulting from algorithm **720** will be modified by algorithm **700** in order to optimize the accuracy of coil layout **800**. FIG. **8**A illustrates coil layout **800** while FIG. **8**B illustrates a planar view of coil layout **800**, which overlaps the traces on the top side and the bottom side of the PCB.

As is illustrated in FIGS. **8**A and **8**B, coil design **800** includes transmission coil **802**, which may include multiple loops and may further include vias through the PCB so that some of the traces for transmission coil **802** is on one side of the PCB while other traces of transmission coil **802** are on the opposite side of the PCB. In some cases, the transmission coil can be optimized to render it as symmetric with respect to the receive coils as possible while minimizing the required space. FIG. **8**A illustrates vias **814** and **816** which allow the traces of transmission coil **802** to be connected between sides of the PCB. As is further illustrated in FIGS. **8**A and **8**B, receive coils include cosine oriented coils **804** and sine oriented coils **806**. Cosine oriented coils **804** include vias **818** that allow transition of the wire traces of cosine oriented coils **804** from one side of the PCB to the other. Similarly, sine oriented coils **806** include vias **820** that allow for transition of wiring for sine oriented coils **806** between sides of the PCB.

Another feature that is included in coil layout **800** are the addition of wells **808**, **810**, and **812** that compensate further for non-uniformity of the fields generated by transmit coils **802** and a resulting offset error generated by that non-uniformity. As is illustrated in coil design **800**, well **808** and **810** are provided to adjust sine oriented coil **804** and well **812** is set to adjust cosine oriented coil **806**. Further, vias **822** and **824** can be provided so that the traces of wells **808** and **812**, respectively, can be on either side of the PCB. Wells **808**, **810**, and **812** can, for example, compensate for offsets in receive coils **804** and **806** due to non-uniformity in the fields generated by transmit coils **802**.

FIGS. **9**A, **9**B, and **9**C illustrate another coil design according to some embodiments of the present invention. As opposed to the linear position system illustrated in coil design **800**, coil design **900** illustrated in FIGS. **9**A, **9**B, and **9**C illustrate a rotary position system. As shown in coil

design **900**, transmission coil **902**, cosine oriented receive coil **904** and sine oriented receiver coil **906** are oriented in a circular fashion. Further, transmission coil **902** includes a distortion portion **916** with leads **920**. Sine oriented receiver coil **906** includes wells **908** and **912** and is connected to a lead **924**. Similarly, cosine oriented receiver coil **904** includes wells **910** and **914** and is coupled to lead **926**. The PCB may also have mounting holes **918**. FIG. **9**A illustrates a planar view of coil design **900** while FIG. **9**B illustrates an angled view of coil design **900** that illustrates vias and traces on both sides of a PCB board on which it is formed. FIG. **9**C illustrates a plan view of coil design **900** on a printed circuit board **930**. Further, a control circuitry **932**, coupled to leads **920**, **924**, and **926**, mounted on circuit board **930**.

FIG. **9**D illustrates the percentage error between the actual position like the one used in positioning system **400**, and the position reconstructed by the simulation by using the RX voltages in, for example, step **704** of algorithm **700**. As illustrated in FIG. **9**D, the percentage error between theoretical and simulated results, after coil design **900** has been optimized according to algorithm **700**, is less than 0.7%. FIG. **9**E illustrates the actual angular position versus the simulated angular position after coil design **900** has been optimized according to algorithm **700**. FIG. **6** illustrates again the percentage of Full Scale error for the optimized coil design **900** after a linearization algorithm has been applied. On that scale, the error is less than 0.3% FS.

Embodiments of the invention include a simulation step **704** that simulates the response of a position locating system coil design and a coil design adjustment algorithm **712** that, using the simulated response, adjusts the coil design for better accuracy. As is discussed above, position sensors suffer from a number of non-idealities. First of all, the field produced by the TX coils is highly non-uniform and because of this non-uniformity the gap between the target and the RX coils allows a lot of magnetic flux not to be correctly shielded by the target. Another effect is that the parts of the RX coils on the bottom of the PCB capture less induced magnetic flux than the corresponding parts in the top of the PCB. Finally, the exits of the RX coils that allow a connection with the controller chip also produce an offset error which is sensible. In the linear and arc sensors, there is additionally the strong effect of the ends of the sensor which produce a huge stray field. This last effect is responsible for most error on the linear and arc designs.

As discussed above, optimization of the coil design begins with a good simulation in step **704** of algorithm **700**. In a first iteration, simulation is performed on the initial coil design input in step **702** of algorithm **700**. In accordance with some embodiments, simulation includes an eddy current solver algorithm developed at the University of Udine, Italy. In particular, an example of a simulation algorithm uses a Boundary Integral Method (BIM), introduced in the publication P. Bettini, R. Specognz, "A boundary integral method for computing eddy currents in thin conductors for arbitrary topology," IEEE Transactions on Magnetics, Vo. 41, No. 3, 7203904, 2015, which provides a very fast simulation (a couple of tens of seconds for 25 target positions). Such an algorithm can be tailored for simulating traces on PCBs and inductive sensor applications. In particular, the simulation can input the geometry of the PCB traces, the geometry of the metallic target, the air gap, the translation/rotation of the metallic target over the coils formed by the traces, and additional fixed conductors that, for example, can be used to simulate ground planes of the PCT or other conductors nearby the sensor. The simulation can output the simulated voltages from receiver coils at a series of positions of the metallic target over the coils.

In some embodiments, a Finite Element Method (FEM) or analogous method may also be used in this application. However, in some cases large amounts of computing time may be needed to perform these simulations. It would be expected that the calculations for each sensor target position may use two or more orders of magnitude of computational time with respect to the BIM method described above. Further, the mesh of the computation domain may need to be rebuilt from scratch for each target position. Furthermore, accuracy in these techniques may be limited since long and thin conductors require a lot of mesh elements to obtain an accurate solution. These calculations may also be limited by memory and computing time resources.

FIG. **10**A illustrates an example of simulation step **704** of algorithm **700**. Algorithm **700** as illustrated in the example of FIG. **7**A, in effect, substantially compensates for the non-ideal effects described above and produces, therefore, the best possible solutions compatible with the physics of the problem of providing an accurate position location system. To accomplish this, a realistic and efficient numerical model of the position locating system is developed. As discussed in more detail below, in some embodiments traces that form transmit coils, receiver coils, and connecting lines are represented with one-dimensional metallic wires. Some embodiments may use more refined simulation algorithms, for example such as brick volumetric elements, partial elements equivalent circuit (PEEC), or an approach based on volume integral formulations, which may provide further enhancement to estimating the magnetic field produced by actual three dimensional current carrying structures. The metallic target can usually be represented by a conducting surface.

As is illustrated in FIG. **10**A, algorithm **704** begins at step **1002**. In step **1002**, the PCB trace design that describes the TX coil and the RX coils, the geometry of the target, the air gap specifications, and the sweep specification is obtained. These input parameters, for example, can be provided by algorithm **700**, either through the initial input during input step **702** of algorithm **700** or from the adjusted coil design from coil adjustment step **712** of algorithm **700**, as is illustrated in FIG. **7**A. Algorithm **704** then proceeds to step **1003**.

In step **1003**, algorithm **704** computes the resistance R and inductance L of the traces of the transmission coil (TX) at the frequency parameter set in step **1002**. The computation is performed without the presence of the target to give an estimation of the quality factor $Q=2\pi fL/R$.

In step **1004**, parameters are set to simulate the performance of a particular coil design and air gap of the coil design received in step **1002** with the metallic target set at a present position as defined in the sweep parameters. If this is the first iteration, the present position is set at the beginning of the sweep defined in the data received in step **1002**. Otherwise, the position is set at the currently defined position in the sweep.

In step **1006**, the electromagnetic fields generated by the transmission coils are determined. The driving voltages and operating frequency for the transmission coils are received with the other parameters provided in step **1002**.

Once the electromagnetic fields from the transmission coil is determined, in step **1008** the eddy currents generated in the metallic target as a result of those fields can be determined. From the eddy currents, the fields generated by the target can be simulated.

In step **1010**, the voltages generated in the receiver coils due to the combination of the fields generated by the transmission coil and the fields generated by the induced eddy currents in the metallic target are determined. In step **1011** the computation of the inductance L is performed again for the present position of the target to evaluate the variation of L with respect to the result of step **1003**. In step **1012**, the response data is stored for future reference.

In step **1014**, algorithm **704** checks to see if the sweep has been completed. If not, then algorithm **704** proceeds to step **1018** where the current position of the metallic target is incremented and then to step **1004** where the simulation with that position is started. If the sweep is completed, algorithm **704** proceeds to step **1016** where the simulation ends and the algorithm returns to step **706** of algorithm **700** illustrated in FIG. **7**A.

Simulations and reconfiguration of the coils according to the simulations (in FIG. **7**A, simulation step **704**, comparison step **706**, decision step **708**, and design adjustment step **712**) should be fast enough to test a large number of coil design configurations in a short period of time. Hundreds, or even thousands, of simulations may be used before an optimized coil design is achieved by algorithm **700**. Consequently, there are some model simplifications that, although not substantially affecting the accuracy of the simulation, can substantially increase the speed. If each simulation takes 10 seconds to complete, for example, an optimization that uses 100 iterations may take 16 minutes. If each simulation takes 10 minutes to complete, however, that same optimization may take 16 hours to complete.

An effective simplification used in some embodiments is to represent the conducting traces used in formation of transmit coils and receiver coils with a one-dimensional wire model. In a worst-case deviation from a one-dimensional wire model, consider a benchmark rectangular trace with a height of 35 μm and a width of 0.3 mm. The rectangular trace can be formed of any non-magnetic conductive material, for example copper. Other metals may be used to form traces, but copper is more typical. The current density of current flowing within the rectangular trace can be very uniform for a section of the trace with thickness on the order of twice the skin depth. For copper, the skin depth is 30 μm at a frequency of 5 MHz. Consequently, for the benchmark rectangular trace discussed above, the current density within the trace will be substantially uniform.

FIG. **10**B illustrates the field generated by a current carrying one-dimensional wire **1020**. There is no difference in the field generated by wire **1020** or by a straight cylinder of a diameter, if the current flowing in the two structures is the same. FIG. **10**C, however, illustrates the field generated around benchmark trace **1022**, which is the benchmark trace described above formed of copper and with height of 35 μm and width of 0.3 mm. As is illustrated in FIG. **10**C, the field even at short distances of less than 1 mm looks the same as that generated by wire **1020** in FIG. **10**B. The difference is in the fields less than about 1 mm from the trace.

FIG. **10**D illustrates the difference between a one-dimensional model of wire **1020** and the benchmark rectangular trace **1022** at a distance of 1 mm from the center of the trace. The representation of a singular rectangular trace **1022** can be realized both with a single-wire and a multi-wire configuration. As can be seen, the field deviates slightly from the one-dimensional model. As can be seen from FIG. **10**D, the error is not negligible, but in both cases it is a small fraction of 1% even at 1 mm. Since most points of the receive coils are much further than 1 mm away with respect to transmission coils, the 1d-wire model may suffice in most applications.

It is also possible to represent the transmission coil with three-dimensional brick shaped elements in which the current density is assumed to be uniform. FIG. **10**E illustrates this approximation. As is illustrated in FIG. **10**E, this reduces the modeling error of the magnetic field produced by the transmission coil by one order of magnitude at a modest additional computational price.

Consequently, in step **1006** and in step **1010**, the traces can be modeled as one-dimensional traces. The source magnetic field produced by the transmit coil is therefore pre-computed by using the 1d-wire model. In some embodiments, more advanced models based on 3D brick elements, which as discussed above can produce roughly the same results, can be used. These models may use a finite-element-matrix form of computations, however such models may need many elements and require a significant increase in computation. As discussed above, FEM-like models may use too many elements (100+millions mesh elements) to reach the precision of the proposed one-dimensional model.

FIG. **10**F illustrates positioning of a metallic target **1204** over receiver coils **1028** and **1026** in a position location system design that is being simulated in algorithm **704**. For purposes of discussion, FIG. **10**F illustrates an example of coil design **800** illustrated in FIGS. **8**A and **8**B, with receiver coils **1028** and **1026** corresponding with the one-dimensional approximation to the traces of receiver coils **804** and **806**, respectively. Transmit coil **802** is not illustrated in FIG. **10**F for simplification of the illustration, but the traces of transmit coil **802** is also approximated by one-dimensional wire traces.

After the electromagnetic fields from the target coil **802** of the position locating system **800** have been simulated, then in step **1008** of the example of algorithm **704** illustrated in FIG. **10**A, the eddy currents of the metallic target **1024** are simulated and the electromagnetic fields that result from those eddy currents are determined. The induced eddy currents in metallic target **1024**, in some embodiments, are computed by an original Boundary Integral Formulation.

Metallic target **1024** can typically be modeled as a thin metal sheet. Usually, metallic target **1024** is thin, 35 μm to 70 μm, while the lateral dimensions are typically measured in millimeters. As discussed above with respect to wire traces, when conductors have a thickness less than about twice the penetration depth of the magnetic field at a particular operating frequency, the induced current density is substantially uniform across the layer thickness. Therefore, the thin conductor of metallic target **1024** can be modeled as a surface in which the induced eddy currents are tangent to the surface. If this is not the case, the more computationally expensive Volumetric Integral Formulations like, the one provided in P. Bettini, M. Passarotto, R. Specogna, "A volume integral formulation for solving eddy current problems on polyhedral messes," IEEE Transactions on Magnetics, Vol. 53, No. 6, 7204904, 2017, or Finite Element modeling can be used to model the target.

As is further illustrated in FIG. **10**F, the surface of metallic target **1024** is represented as covered by mesh elements **1026**. Mesh elements **1026** are non-overlapping polygons, typically triangular, that cover the entire surface of metallic target **1024** and form a discrete surface.

Once the simulation on metallic target **1024** is performed in step **1008** of **704**, as illustrated in FIG. **10**A, then in step **1010** the response of receiver coils **804** and **806** is simulated. As is further illustrated in algorithm **704**, simulation **704**

sweeps the target across position locator system **800** and estimates "in silico" the voltages on the receive coils **804** and **806** for all specified positions of the target **1024**.

As is further illustrated in step **712** of algorithm **700** illustrated in FIG. **7**A, the shape of receive coils **804** and **806**, assuming that transmit coil is adapted in the best possible way to all non-idealities of the sensor **800** at the same time. This represents the best solution, given that the non-idealities cannot be all removed and as discussed above several approximations are used in simulation algorithm **704**.

FIG. **11** illustrates an example of algorithm **712**. In algorithm **712**, the centerline of the receive coils **804** and **806** traces and transmit coil **802** are represented as one-dimensional pathways. Splines or any other interpolation function can be used to link the one-dimensional pathways to form the shape of transmit coil **802** and receive coils **804** and **806**. More efficiently, the distortion of the receive coils may be realized by the application of a suitable function. For example, in the rotary sensor the function will be a function of the radius. In step **1102**, the current coil design layout, the simulation results, and in some cases the comparison provided in step **706** are input and received in algorithm **712**. A non-linear programming solver can then be used to find the shape of transmit coil **802** and receive coils **804** and **806** that minimize a given objective function. The objective function is formed by three parts as illustrated in FIG. **11**. In step **1103** the width of the external wells **1402** and **1404** illustrated in FIG. **14** is established in order to minimize the offset without the target. In step **1104**, the root mean square of error (RMS) between the detected position (i.e. the electrical angle) and the ideal one is minimized. This does not impose anything about the shape of the voltage V_{cos} and V_{sin} with respect to position. In step **1106**, algorithm **712** evaluates the RMS of the difference between two sinusoids with equal amplitude and the simulated values of V cos and V sin as a function of position in order to constrain the shape of the output voltages. In some embodiments, the shape of the redesigned receive coils **804** and **806** may converge in both steps **1104** and **1106**. In step **1108**, the new coil layout is output.

In some embodiments, steps **1104** and **1106** may use Metaheuristic optimization solvers. Metaheuristic optimization solvers tend to be very slow, however. Therefore, in some embodiments metaheuristic global searching technique like genetic algorithms or particle swarm algorithms can be used. In some embodiments, a deterministic algorithm like the interior point method or the trust region algorithm can be used in steps **1104** and **1106**. In particular, since initial starting designs for receive coils **804** and **806** can be standard sine and cosine profiles, and the resulting optimized design should result in a small perturbation of the initial design, then it is expected that local search methods can be used to sufficiently find the global minima resulting in optimal designs. The basics of optimization theory can be found, for example, in S. S. Rao, Engineering Optimization: Theory and Practice, John Wiley & Sons, 2009.

FIG. **12** illustrates another embodiment of algorithm **712**. The input provided in step **1202** is the same as that discussed with respect to step **1102** of FIG. **11**. In step **1204**, the transmission coil (TX) is automatically generated providing the maximum symmetry and reducing the space required.

An example transmission coil that can result is shown in FIG. **13** where the trace deviation **1304** is computed according to the PCB specifications in term of trace to trace distance and vias dimensions (pad radius). Moreover, a reduction of the space can be obtained with the alternate vias positioning **1302**.

In the embodiment of algorithm **712** illustrated in FIG. **12**, the algorithm adjusts the sine receive coil and the cosine receive coil is defined relative to the modified sine receive coil. One skilled in the art will recognize that instead of modifying the sine receive coil, the cosine receive coil could be modified instead and the sine receive coil defined relative to the cosine receive coil. For illustrative purposes, FIG. **13** illustrates the modification **1300** of a sine receive coil as described with respect to FIG. **12**.

Receiving coils (RX) design can be defined with a double loop iteration. Initially, in step **1206**, the sine shaped RX coil **1316** is symmetrically partially extended along x direction (with the reference system **1314**) as in trace **1310** to compensate the flux leakage due to the target non-idealities. With the imposed coil extension, in step **1208** the sine shaped coil **1316** is then deformed along y direction as in trace **1312** using a proper displacement function acting on all the points of the coil **1316**. Given these settings, in step **1210** the algorithm computes the position of the vias. The vias position **1308** is established according with information specified in step **1202** and in order to eliminate the signal mismatch previously mentioned. Voltage mismatch appears whenever there are more vias in one receiver coil than there are in the other receiver coil or the vias are positioned in an unbalanced way (i.e. not symmetric). The voltage mismatch that results is a greater peak-to-peak amplitude of the sine signal with respect to the cosine signal (or vice versa) when the target is moving. To achieve the goal of reducing voltage mismatch, the vias are designed in such a way that the length of the parts of the SIN (**1316**) and COS (**1318**) RX coils in the bottom of the PCB is the same. Moreover, the vias are symmetric with respect to the symmetry center of the design.

In step **1212**, the sine and cosine receive coil traces are defined. In some embodiments, a one-dimensional model is used to define the traces.

In step **1214**, algorithm **712** computes the offset without the target and in step **1216** if the minimum offset criterion is not satisfied the algorithm restarts from step **1208** after modifying the sine RX extension in step **1224**. When the minimum offset is reached the algorithm proceeds to step **1218**, evaluating the voltages as described in FIG. **10**A and then computing the maximum error between the ideal and the simulated positions. If the lowest possible error is not reached in step **1220**, the algorithm goes back to step **1206** after modifying the sine RX amplitude in step **1222**, providing another configuration. Once the lowest error for the current input is obtained the algorithm ends at return step **1226**.

In some embodiments the offset without target compensation is realized without the presence of the wells as illustrated in FIG. **13**. Anyway, the design symmetry is always guaranteed thanks to the balanced extensions **1306** and **1307** of the sine shaped **1316** and cosine shaped **1318** RX coils.

The above detailed description is provided to illustrate specific embodiments of the present invention and is not intended to be limiting. Numerous variations and modifications within the scope of the present invention are possible. The present invention is set forth in the following claims.

What is claimed is:

1. A method of providing an optimized position locating sensor coil design, comprising:

receiving into a computing system a coil design and a desired specification for the accuracy of the position locating sensor coil design, the coil design being represented in a datafile to provide transmit coil, sine coil, and cosine coil coordinates;

simulating, in the computing system, position determination over a range of positions of a metallic target with respect to the coil design to form a simulated performance of the coil design, the simulated performance representing the simulated response of the sine coil and cosine coil to the metal target excited by the transmit coil over the range of positions;

comparing, in the computer system, the simulated response with the desired specification for the accuracy to provide a comparison;

modifying, in the computer system, the coil design based on the comparison between the simulated performance and the desired specification to arrive at an updated coil design that performs closer to the desired specification for the accuracy; and

providing the updated coil design;

wherein the coil design and the updated coil design includes a transmit coil layout, a sine receive coil layout, a cosine receive coil layout, a metallic target geometry, a sweep geometry, and an air gap, and

wherein simulating position determination includes, for each of a set of positions within the range of positions of a metallic target over the coil design,

computing parameters for the transmit coil in the absence of the sine receive coil and the cosine receive coil;

determining an electromagnetic field produced by the transmit coil;

determining eddy currents induced in the metallic target by the electromagnetic field produced by the transmit coil at a present location from the set of positions of the target;

determining a response of the sine receiver coil and the cosine receiver coil produced by the eddy currents in the metallic target;

computing a second set of parameters for the transmit coil with the metallic target; and

storing the voltage signals as a function of the position of the metallic target.

2. The method of claim **1**, further including:

repeating the simulating, comparing, and modifying steps on the updated coil designs to arrive at a final coil design with optimized performance that meets the desired specification for the accuracy; and

providing the final design for printing on a printed circuit board.

3. The method of claim **1**, wherein determining eddy currents includes simulating the metallic target with a boundary-integral-method.

4. The method of claim **1**, further including:

physically producing a position locating system according to the final design; and

validating the position locating system against simulated results of the stored voltage signals.

5. A method of providing an optimized position locating sensor coil design, comprising:

receiving into a computing system a coil design and a desired specification for the accuracy of the position locating sensor coil design, the coil design being represented in a datafile to provide transmit coil, sine coil, and cosine coil coordinates;

simulating, in the computing system, position determination over a range of positions of a metallic target with respect to the coil design to form a simulated performance of the coil design, the simulated performance representing the simulated response of the sine coil and cosine coil to the metal target excited by the transmit coil over the range of positions;

comparing, in the computer system, the simulated response with the desired specification for the accuracy to provide a comparison;

modifying, in the computer system, the coil design based on the comparison between the simulated performance and the desired specification to arrive at an updated coil design that performs closer to the desired specification for the accuracy; and

providing the updated coil design,

wherein the coil design and the updated coil design includes a transmit coil layout, a sine receive coil layout, a cosine receive coil layout, a metallic target geometry, a sweep geometry, and an air gap, and

wherein each of the receive coils includes one or more wells.

6. The method of claim **5**, further including:

repeating the simulating, comparing, and modifying steps on the updated coil designs to arrive at a final coil design with optimized performance that meets the desired specification for the accuracy; and

providing the final design for printing on a printed circuit board.

7. The method of claim **5**, further including:

physically producing a position locating system according to the final design; and

validating the position locating system against simulated results of the stored voltage signals.

8. A method of providing an optimized position locating sensor coil design, comprising:

receiving into a computing system a coil design and a desired specification for the accuracy of the position locating sensor coil design, the coil design being represented in a datafile to provide transmit coil, sine coil, and cosine coil coordinates;

simulating, in the computing system, position determination over a range of positions of a metallic target with respect to the coil design to form a simulated performance of the coil design, the simulated performance representing the simulated response of the sine coil and cosine coil to the metal target excited by the transmit coil over the range of positions;

comparing, in the computer system, the simulated response with the desired specification for the accuracy to provide a comparison;

modifying, in the computer system, the coil design based on the comparison between the simulated performance and the desired specification to arrive at an updated coil design that performs closer to the desired specification for the accuracy; and

providing the updated coil design,

wherein the coil design and the updated coil design includes a transmit coil layout, a sine receive coil layout, a cosine receive coil layout, a metallic target geometry, a sweep geometry, and an air gap, and

wherein traces of the transmit coil and traces of the receive coils are treated as one-dimensional wires.

9. The method of claim **8**, further including:

repeating the simulating, comparing, and modifying steps on the updated coil designs to arrive at a final coil design with optimized performance that meets the desired specification for the accuracy; and

providing the final design for printing on a printed circuit board.

10. The method of claim **8**, further including:

physically producing a position locating system according to the final design; and

validating the position locating system against simulated results of the stored voltage signals.

11. A method of providing an optimized position locating sensor coil design, comprising:

receiving into a computing system a coil design and a desired specification for the accuracy of the position locating sensor coil design, the coil design being represented in a datafile to provide transmit coil, sine coil, and cosine coil coordinates;

simulating, in the computing system, position determination over a range of positions of a metallic target with respect to the coil design to form a simulated performance of the coil design, the simulated performance representing the simulated response of the sine coil and cosine coil to the metal target excited by the transmit coil over the range of positions;

comparing, in the computer system, the simulated response with the desired specification for the accuracy to provide a comparison;

modifying, in the computer system, the coil design based on the comparison between the simulated performance and the desired specification to arrive at an updated coil design that performs closer to the desired specification for the accuracy; and

providing the updated coil design,

wherein the coil design and the updated coil design includes a transmit coil layout, a sine receive coil layout, a cosine receive coil layout, a metallic target geometry, a sweep geometry, and an air gap, and

wherein modifying the coil design comprises:

establishing well amplitude for the sine receive coil and the cosine receive coil;

minimizing a root mean square (RMS) error between a simulated position and an ideal position;

evaluating a root mean square distance between sinusoids and the simulated cosine and sine voltages; and

providing the updated coil design.

12. The method of claim **11**, minimizing the RMS error and the RMS distance is accomplished with a metaheuristic optimization solver.

13. The method of claim **11**, further including:

repeating the simulating, comparing, and modifying steps on the updated coil designs to arrive at a final coil design with optimized performance that meets the desired specification for the accuracy; and

providing the final design for printing on a printed circuit board.

14. The method of claim **11**, further including:

physically producing a position locating system according to the final design; and

validating the position locating system against simulated results of the stored voltage signals.

15. A method of providing an optimized position locating sensor coil design, comprising:

receiving into a computing system a coil design and a desired specification for the accuracy of the position locating sensor coil design, the coil design being represented in a datafile to provide transmit coil, sine coil, and cosine coil coordinates;

simulating, in the computing system, position determination over a range of positions of a metallic target with respect to the coil design to form a simulated performance of the coil design, the simulated performance representing the simulated response of the sine coil and cosine coil to the metal target excited by the transmit coil over the range of positions;

comparing, in the computer system, the simulated response with the desired specification for the accuracy to provide a comparison;

modifying, in the computer system, the coil design based on the comparison between the simulated performance and the desired specification to arrive at an updated coil design that performs closer to the desired specification for the accuracy; and

providing the updated coil design,

wherein the coil design and the updated coil design includes a transmit coil layout, a sine receive coil layout, a cosine receive coil layout, a metallic target geometry, a sweep geometry, and an air gap, and

wherein modifying the coil design comprises:

generating a symmetric transmit coil layout with minimum space;

extending a receive coil according to a boundary flux leakage;

setting the receive coil amplitude according to an offset;

calculating symmetric via positions that avoids a voltage mismatch;

defining coil traces for the receive coil and a second receive coil; and

calculating an offset without the presence of the target.

16. The method of claim **15**, further including:

checking minimum offset criteria; and

modifying the amplitude of the receive coil if the minimum is not met.

17. The method of claim **16**, further including if the minimum offset criteria is met, evaluating the maximum error and modifying the receive coil design if the lowest criteria is not met.

18. The method of claim **15**, further including:

repeating the simulating, comparing, and modifying steps on the updated coil designs to arrive at a final coil design with optimized performance that meets the desired specification for the accuracy; and

providing the final design for printing on a printed circuit board.

19. The method of claim **15**, further including:

physically producing a position locating system according to the final design; and

validating the position locating system against simulated results of the stored voltage signals.

* * * * *